

PROCEEDINGS OF SPIE

# ***Optoelectronic Integrated Circuits X***

**Louay A. Eldada  
El-Hang Lee**  
*Editors*

**21–23 January 2008  
San Jose, California, USA**

*Sponsored and Published by*  
SPIE

**Volume 6897**

Proceedings of SPIE, 0277-786X, v. 6897

SPIE is an international society advancing an interdisciplinary approach to the science and application of light.

The papers included in this volume were part of the technical conference cited on the cover and title page. Papers were selected and subject to review by the editors and conference program committee. Some conference presentations may not be available for publication. The papers published in these proceedings reflect the work and thoughts of the authors and are published herein as submitted. The publisher is not responsible for the validity of the information or for any outcomes resulting from reliance thereon.

Please use the following format to cite material from this book:

Author(s), "Title of Paper," in *Optoelectronic Integrated Circuits X*, edited by Louay A. Eldada, El-Hang Lee, Proceedings of SPIE Vol. 6897 (SPIE, Bellingham, WA, 2008) Article CID Number.

ISSN 0277-786X

ISBN 9780819470720

Published by

**SPIE**

P.O. Box 10, Bellingham, Washington 98227-0010 USA

Telephone +1 360 676 3290 (Pacific Time) · Fax +1 360 647 1445

SPIE.org

Copyright © 2008, Society of Photo-Optical Instrumentation Engineers

Copying of material in this book for internal or personal use, or for the internal or personal use of specific clients, beyond the fair use provisions granted by the U.S. Copyright Law is authorized by SPIE subject to payment of copying fees. The Transactional Reporting Service base fee for this volume is \$18.00 per article (or portion thereof), which should be paid directly to the Copyright Clearance Center (CCC), 222 Rosewood Drive, Danvers, MA 01923. Payment may also be made electronically through CCC Online at [copyright.com](http://copyright.com). Other copying for republication, resale, advertising or promotion, or any form of systematic or multiple reproduction of any material in this book is prohibited except with permission in writing from the publisher. The CCC fee code is 0277-786X/08/\$18.00.

Printed in the United States of America.

Publication of record for individual papers is online in the SPIE Digital Library.

**SPIE**   
Digital Library

[SPIDigitalLibrary.org](http://SPIDigitalLibrary.org)

---

**Paper Numbering:** Proceedings of SPIE follow an e-First publication model, with papers published first online and then in print and on CD-ROM. Papers are published as they are submitted and meet publication criteria. A unique, consistent, permanent citation identifier (CID) number is assigned to each article at the time of the first publication. Utilization of CIDs allows articles to be fully citable as soon they are published online, and connects the same identifier to all online, print, and electronic versions of the publication. SPIE uses a six-digit CID article numbering system in which:

- The first four digits correspond to the SPIE volume number.
- The last two digits indicate publication order within the volume using a Base 36 numbering system employing both numerals and letters. These two-number sets start with 00, 01, 02, 03, 04, 05, 06, 07, 08, 09, 0A, 0B ... 0Z, followed by 10-1Z, 20-2Z, etc.

The CID number appears on each page of the manuscript. The complete citation is used on the first page, and an abbreviated version on subsequent pages. Numbers in the index correspond to the last two digits of the six-digit CID number.

# Contents

vii Conference Committee

ix Introduction

*Papers from Conference 6899 Joint Sessions*

xi *Low-cost high-density optical parallel link modules and optical backplane for the last 1-meter regime applications (Invited Paper) [6899-01]*  
*T. Mikawa, National Institute of Advanced Industrial Science and Technology (Japan)*

xxi *Fully embedded board level optical interconnects: from point-to-point interconnection to optical bus architecture (Invited Paper) [6899-02]*  
*X. Wang, Omega Optics Inc. (USA); R. T. Chen, Univ. of Texas at Austin (USA)*

xxxi *Towards flexible routing schemes for polymer optical interconnections on printed circuit boards [6899-03]*  
*N. Hendrickx, G. Van Steenberge, E. Bosman, Ghent Univ. (Belgium); J. Van Erps, H. Thienpont, Vrije Univ. Brussel (Belgium); P. Van Daele, Ghent Univ. (Belgium)*

---

## SESSION 1 TRENDS IN OEICs

---

6897 03 **High-index-contrast chalcogenide waveguides (Invited Paper) [6897-02]**  
C. K. Madsen, M. Solmaz, R. Atkins, Texas A&M Univ. (USA)

6897 05 **Ultra-high resolution and compact volume holographic spectrometers (Invited Paper) [6897-04]**  
A. Adibi, C. Hsieh, O. Momtahan, M. Badieirostami, Georgia Institute of Technology (USA)

---

## SESSION 2 NANOENGINEERED OEICs

---

6897 0A **Analysis of a novel micro surface plasmon resonance sensor with attenuated total reflection mirror [6897-09]**  
G.-Y. Oh, D.-G. Kim, W.-K. Choi, Y.-W. Choi, Chung-Ang Univ. (South Korea)

6897 0B **Coupling performance and fabrication method of a waveguide grating coupler with non-uniform duty ratio [6897-10]**  
J. S. Yang, J.-H. Sung, B. O, S. G. Lee, E.-H. Lee, Inha Univ. (South Korea)

---

## SESSION 3 HYBRID OEICs

---

6897 0E **Chip scale integrated planar photonics (Invited Paper) [6897-13]**  
N. M. Jokerst, Duke Univ. (USA); S.-Y. Cho, New Mexico State Univ. (USA); M. A. Brooke, L. Luan, Duke Univ. (USA)

---

**SESSION 4 OPTICAL INTERCONNECT TECHNOLOGIES I: JOINT SESSION WITH CONFERENCE 6899**

---

- 6897 OG **Er<sub>x</sub>Y<sub>2-x</sub>SiO<sub>5</sub> nanocrystal and thin film for high gain per length material** [6897-15]  
K. Suh, H. Go, S.-Y. Lee, J. S. Chang, M.-S. Yang, J. H. Shin, Korea Advanced Institute of Science and Technology (South Korea)

---

**SESSION 5 OPTICAL INTERCONNECT TECHNOLOGIES II: JOINT SESSION WITH CONFERENCE 6899**

---

- 6897 OI **Comparison of bandwidth limits for on-card electrical and optical interconnects for 100 Gb/s and beyond (Invited Paper)** [6897-17]  
P. Pepeljugoski, M. Ritter, J. A. Kash, F. Doany, C. Schow, Y. Kwark, L. Shan, D. Kam, X. Gu, C. Baks, IBM T. J. Watson Research Ctr. (USA)
- 6897 OJ **Driver-receiver combined optical transceiver modules for bidirectional optical interconnection (Invited Paper)** [6897-18]  
H.-H. Park, S.-K. Kang, D.-W. Kim, N. T. H. Nga, S.-H. Hwang, T.-W. Lee, Information and Communications Univ. (South Korea)

---

**SESSION 6 SILICON OEICs**

---

- 6897 OL **Monolithic integration of photonic and electronic circuits in a CMOS process (Invited Paper)** [6897-20]  
A. Mekis, S. Abdalla, B. Analui, S. Gloeckner, A. Guckenberger, R. Koumans, D. Kucharski, Y. Liang, G. Masini, S. Mirsaidi, A. Narasimha, T. Pinguet, V. Sadagopan, B. Welch, J. White, J. Witzens, Luxtera (USA)
- 6897 ON **Materials and devices for compact optical amplification in Si photonics (Invited Paper)** [6897-22]  
J. H. Shin, M.-S. Yang, J.-S. Chang, S.-Y. Lee, K. Suh, Korea Advanced Institute of Science and Technology (South Korea); H. G. Yoo, Univ. of Rochester (USA); Y. Fu, Institute of Optics, Univ. of Rochester (USA); P. Fauchet, Univ. of Rochester (USA)
- 6897 OO **Fabrication and characterization of Er doped silicon-rich silicon nitride(SRSN) micro-disks** [6897-23]  
J. S. Chang, M.-K. Kim, Y.-H. Lee, J. H. Shin, Korea Advanced Institute of Science and Technology (South Korea); G. Y. Sung, Electronics and Telecommunications Research Institute (South Korea)

---

**SESSION 7 POLYMER AND ORGANIC-INORGANIC OEICs**

---

- 6897 OS **Polymer-cladded athermal high-index-contrast waveguides** [6897-42]  
W. N. Ye, J. Michel, L. C. Kimerling, Massachusetts Institute of Technology (USA); L. Eldada, DuPont Photonics Technologies (USA)

---

**SESSION 8 SENSING AND IMAGING OEICs**

---

- 6897 0U **Optical performance of bare image sensor die and sensors packaged at the wafer level and protected by a cover glass** [6897-28]  
G. Humpston, Tessera U.K. (United Kingdom); A. Grinman, Tessera Israel (Israel); O. Jackl, M. Ebel, Schott AG (Germany)
- 6897 0V **Mega-pixel PQR laser chips for interconnect, display ITS, and biocell-tweezers OEIC (Invited Paper)** [6897-29]  
O. Kwon, J. H. Yoon, D. K. Kim, Y. C. Kim, S. E. Lee, S. S. Kim, Pohang Univ. of Science and Technology (South Korea)
- 6897 0W **Design of a silicon optical micro-ring resonator sensor for improved sensitivity and selectivity** [6897-30]  
H.-S. Lee, B. H. O, S. G. Lee, E.-L. Lee, Inha Univ. (South Korea)

---

**SESSION 9 SWITCHING AND MODULATION OEICs**

---

- 6897 0X **Semiconductor optical amplifier switch matrices for optical header recognition (Invited Paper)** [6897-31]  
M. Dagenais, G. Ryu, S. Saini, Univ. of Maryland, College Park (USA); F. Toudeh-Fallah, R. Gyurek, P. Donner, Cisco Systems Inc. (USA)
- 6897 0Y **Metro area network optical routers and technologies: FOADM, BOADM, ROADM, and TOADM (Invited Paper)** [6897-32]  
L. Eldada, DuPont Photonics Technologies (USA)
- 6897 0Z **10 GHz dual loop opto-electronic oscillator without RF-amplifiers** [6897-33]  
W. Zhou, Army Research Lab. (USA); O. Okusaga, Army Research Lab. (USA) and Univ. of Maryland, Baltimore County (USA); C. Nelson, D. Howe, National Institute of Standards and Technology (USA); G. Carter, Univ. of Maryland, Baltimore County (USA)
- 6897 10 **Wavelength-dependence transmission experiment of feedforward optical transmitter using light injection technique in WDM/SCM radio-over-fiber system** [6897-34]  
Y. T. Moon, J. W. Jang, W.-K. Choi, Y.-W. Choi, Chung-Ang Univ. (South Korea)

---

**POSTER SESSION**

---

- 6897 11 **Photonic crystal-based GE-PON triplexer using point defects** [6897-35]  
D.-S. Park, B.-H. O, S.-G. Park, E.-H. Lee, S. G. Lee, Inha Univ. (South Korea)
- 6897 13 **Bio-signal processing using a novel lock-in detection technique for the portable bio-optical systems** [6897-37]  
I.-I. Jung, D. G. Kim, W.-K. Choi, D.-G. Kim, Y.-W. Choi, Chung-Ang Univ. (South Korea)
- 6897 17 **The effect of KOH and KOH/IPA etching on the surface roughness of the silicon mold used for polymer waveguide imprinting** [6897-41]  
S. An, S.-G. Lee, B.-H. O, H.-H. Kim, S.-G. Park, E.-H. Lee, Inha Univ. (South Korea)

*Author Index*



# Conference Committee

## *Symposium Chair*

**Ali Adibi**, Georgia Institute of Technology (USA)

## *Symposium Cochair*

**James G. Grote**, Air Force Research Laboratory (USA)

## *Program Track Chair*

**Yakov Sidorin**, Photineer Technology Group (USA)

## *Conference Chairs*

**Louay A. Eldada**, DuPont Photonics Technologies (USA)

**El-Hang Lee**, Inha University (South Korea)

## *Program Committee*

**Yung Jui Chen**, University of Maryland, Baltimore County (USA)

**Larry A. Coldren**, University of California, Santa Barbara (USA)

**Yeshaiahu Fainman**, University of California, San Diego (USA)

**Alexei L. Glebov**, Finisar Corporation (USA)

**Hans J. Heider**, Technische Universität Hamburg-Harburg (Germany)

**Ghassan E. Jabbour**, Arizona State University (USA)

**Richard M. Osgood**, Columbia University (USA)

**Manijeh Razeghi**, Northwestern University (USA)

**Giancarlo C. Righini**, Istituto di Fisica Applicata Nello Carrara (Italy)

**Robert Scarmozzino**, RSoft Design Group, Inc. (USA)

## *Session Chairs*

- 1 Trends in OEICs  
**Louay A. Eldada**, DuPont Photonics Technologies (USA)
- 2 Nanoengineered OEICs  
**Giancarlo C. Righini**, Istituto di Fisica Applicata Nello Carrara (Italy)
- 3 Hybrid OEICs  
**Jung Hoon Shin**, Korea Advanced Institute of Science and Technology (South Korea)
- 4 Optical Interconnect Technologies I: Joint Session with Conference 6899  
**Alexei L. Glebov**, Finisar Corporation (USA)

- 5 Optical Interconnect Technologies II: Joint Session with Conference 6899  
**Louay A. Eldada**, DuPont Photonics Technologies (USA)
- 6 Silicon OEICs  
**Richard M. Osgood**, Columbia University (USA)
- 7 Polymer and Organic-Inorganic OEICs  
**Louay A. Eldada**, DuPont Photonics Technologies (USA)
- 8 Sensing and Imaging OEICs  
**Mario Dagenais**, University of Maryland, College Park (USA)
- 9 Switching and Modulation OEICs  
**Manijeh Razeghi**, Northwestern University (USA)



## Introduction

This volume features contributions from scientists and engineers in the general area of optoelectronic integrated circuits (OEICs). The joint session between the OEIC conference and the Photonics Packaging, Integration, and Interconnects conference this year resulted in valuable contributions in the areas of OEIC packaging and board-level/chip-to-board/intra-chip interconnects.

Optical, electronic, and biological devices are integrated to address the issues of cost, space, performance, and reliability. Demands for greater bandwidths have driven the telecom and datacom research communities to realize complex OEICs such as transceivers, low-chirp optical sources, switching systems, and multi-channel optical distribution systems. The integration of multi-wavelength laser arrays, monitoring photodiodes, and drivers is becoming a reality in the communications arena. Other emerging OEIC application areas include all-optical packet switching, neural systems, optical computing, optical storage, smart pixel arrays, projection displays, imaging, scanning, printing, medical diagnosis, and chemical/biological sensing.

The increased level of integration in recent years has resulted in an increased level of miniaturization. The scientific and technological issues and challenges concerning the micro/nano/quantum-scale integration of optoelectronic devices, circuits, components, modules, subsystems, and systems include the size effect, proximity effect, energy confinement effect, microcavity effect, single photon effect, optical interference effect, high field effect, nonlinear effect, noise effect, quantum optical effect, and chaotic noise effects. Optical alignment between miniature devices, minimizing interconnection and coupling losses, and maintaining the stability of optical interfaces, are some of the important issues that are receiving careful consideration.

Papers in these proceedings include discussions of the physics, theory, design, modeling, simulation, and scaling of a wide range of OEICs with regard to their optical, electrical, thermal, and mechanical properties; the integration of different optoelectronic structure types including dots, wells, planar, free space, one-dimensional, two-dimensional, and three-dimensional photonics crystals; the integration of different functions including lasers, amplifiers, detectors, sensors, modulators, isolators, circulators, electrically actuated/all-optical switches, attenuators, couplers, multi/demultiplexers, filters, wavelength converters, polarization controllers, chromatic/polarization mode dispersion compensators, intra-chip/chip-to-board/board-level optical interconnects, and control electronics; the fabrication, processing, and manufacturing techniques (UV/deep UV/x-ray/e-beam lithography, casting, molding, embossing, etching, passivation, etc.), as well as the packaging, assembly, reliability and qualification of monolithic and hybrid OEICs in a variety of materials (semiconductors, silica,

polymers, ferroelectrics, magnetics, metals, biomaterials, etc.). Some papers describe the refinement of existing schemes and processes, while others introduce novel concepts and new designs. Papers from academic and research institutions push the state of the art in miniaturization, level of integration, and performance figures of merit, and papers from the industry emphasize design criteria and manufacturing methods that result in practical OEICs that can be deployed commercially today or in the near future.

Although this volume cannot include all the recent important work in the vast field of OEICs, it does cover a significant cross-section of the advances happening globally in areas where OEICs are making an impact, and it provides a roadmap to the future of OEICs by presenting the cutting-edge work and the visions of leading experts who are actively inventing the future.

**Louay Eldada**  
**El-Hang Lee**

# Low-cost, high-density optical parallel link modules and optical backplane for the last 1 meter regime applications

Takashi Mikawa

National Institute of Advanced Industrial Science and Technology (AIST)  
 Opto-Electronic System Integration Collaborative Research Team  
 NeRI, AIST Tsukuba Central 2, 1-1-1, Umezono, Tsukuba, Ibaraki, 305-8568, Japan  
 (e-mail: [t-mikawa@aist.go.jp](mailto:t-mikawa@aist.go.jp)).

## ABSTRACT

We describe our R & D on optoelectronic packaging technologies such as the optical backplane utilizing 300 pieces of the high index contrast fine multimode fibers and the low-cost and high-density OE-conversion parallel link modules operating at 10 Gbps /ch for less than 1 m regime applications. Combination of the developed backplane and the modules implies potential of 3 Tbps aggregate throughputs at the board-to-board level optical interconnections. We also introduce novel component technologies for low-cost and high-density optical coupling between optical devices. These technologies include the monolithic two wavelengths twin VCSELs and easy self-alignment coupling technology capable of alleviating difficulties for optics penetration inside the box.

**Keywords:** optical backplane, optical parallel link module, monolithic VCSEL, optical coupling, self-alignment, low-cost, high-density, packaging, 40,100 GbEther systems, intra box

## 1. INTRODUCTION

Rapid increase in broadband network demands has led to the explosive capacity of the information throughputs for the inter and intra boxes applications. One of the prospects suggests that total data rates inside the boxes such as high-end routers and some commodity machines i.e. next generation games, computer graphics equipments will reach over 10 Tbps around the year of 2010[1],[2]. In order to cope with these high-capacity throughputs, optics will play important role to avoid the existing I/O bottleneck of the conventional copper metal wiring around high-capacity switching LSIs of servers and routers, and around electrical connectors between interface board and backplane. Figure 1 shows schematic of the server and router boxes, where in the optics case, optical backplane, interface boards, optical multi-channel connectors joining backplane and boards and optical modules to be assembled on the board will be essential key components to construct the whole body of the boxes. Regarding the backplane and board with the multi-channel optical connector, various types of the configurations are reported utilizing the polymer waveguide [3 ][4] [5], [6],[7] polymer optical fibers (POF) [8 ], and silica optical fibers [9 ],[10],[11]. Of these many kinds of approaches, the fiber based backplane will be one of the promising candidates for practical realization, because of the well established silica fiber technology and because of the low-loss optical transmission characteristics to be beneficial to obtain the large link loss budget of the board-to-board interconnect systems via backplane. The standardization viewpoint will also be important for the manufactured optical backplane to be compatible to the existing commercial base cabinets [12 ]. As for the optical modules, to meet high-capacity requirements of the high-end routers and servers, development of the high-density and low-cost OE modules [13 ],[14 ] suited for the next generation 40 and 100 GbEther systems [15],[16] will be crucial. Cost-effective design of the modules to place emphasis on the assembling cost reduction based on the easy optical coupling techniques as well as high-performances is indispensable.

In the present paper, the fiber based optical backplane and the 4 x 10 Gbps optical modules for less than 1 m regime intra boxes applications are described in section 2 [10],[11]. In paragraph 3-1 of section3, low-cost and high-density optical modules having over 100 Gbps throughputs are presented [17]. In paragraph 3-2 of section3, optical module component technologies including the monolithic two wavelengths twin VCSELs [18] and self-alignment optical coupling technology [19] for low-cost and high-density packaging are discussed. Finally, the conclusions are given in section 4.

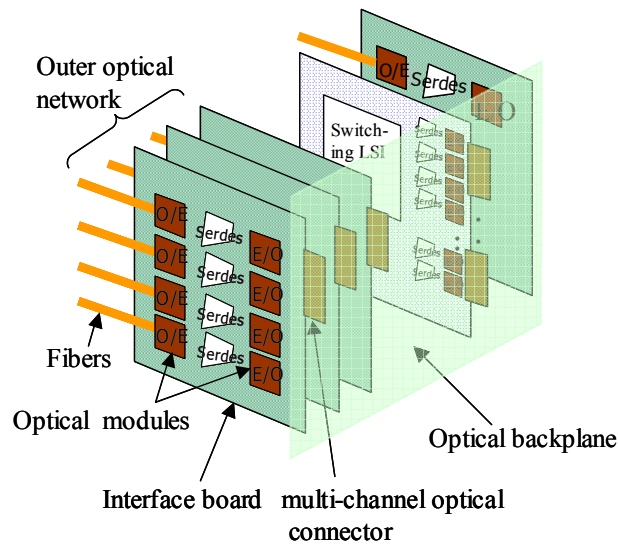


Fig. 1. Schematic illustration of server and router boxes

## 2. OPTICAL BACKPLANE WITH MULTI-CHANNEL CONNECTORS AND 4 X 10 Gbps OPTICAL MODULES

With increase of switching capacity, switching (SW) LSI I/O bottleneck, that is, LSI pin count bottleneck occurs from around 1 Tbps in the copper metal wiring due to the differential pair and ground etc[20]. Also, backplane switching connector width becomes too large for practical use from around several Tbps in the case of the copper metal, due to rather wide electrical connector pitch of about 1 mm[20]. High-speed and high-density optical signals for example 10-40Gbps/ch, will enable drastic reduction of the SW LSI pin counts and SW connector width of the backplane to solve the above mentioned copper metal bottlenecks. Therefore, backplane utilizing the optics will be very useful for the next generation multi-terabit routers and servers.

We have developed the optical backplane with the same board size as the electrical Advanced-TCA (ATCA) de-facto standard [10],[11] [12]. By adopting standardization viewpoint, we expect to accelerate penetration of this kind of optical backplane to the commercial fields. Target aggregate throughputs are 3 Tbps, five times higher than existing ATCA electrical backplane. If signal speed/ch is 10 Gbps, a total of 300 pieces of the fiber should be contained to realize 3 Tbps throughputs. Figure 2 shows photograph of the fabricated backplane having multi-channel MT connectors to mate with interface boards with a slot pitch of 30 mm. The backplane is designed to be housed into the box of the ATCA compliant size of 483mm(W)x418mm(H)x378mm(D). Dual star configuration is adopted to assemble the two switching boards in the middle of the backplane for redundancy. A total of 300 pieces of multimode fiber is contained in the polyimide sheets. Fiber bending radius is designed to be as small as 5 mm for high-density wiring pattern layout. Two fiber sheets with MT-like ferrules are overlapped to build left and right side of the optical backplane, respectively. Even in the optics case, backside fiber contingency of the boxes sometimes occurs. But this contingency is much improved by using the fabricated optical backplane.

To construct high-density optical backplane, we have developed the following component technologies:(1)Small diameter, high index contrast ( $\Delta$ ) fine fiber ,(2)Small sized connector housing technologies, both(1) and (2) for high-capacity, and (3) Assembling technique to build ferruled fiber without removal of the fiber resin coating and MTP/PIPE (MT ferrules with Pre-Installed, Pre-polished both Ends fibers) technology for cost reduction. Other than these technologies, standardization and maintenance techniques will also be important. Figure 3 shows schematic of the developed fiber with small diameter and high  $\Delta$ . The outer diameter is as small as 125  $\mu$ m with conventional core size of 50  $\mu$ m. Refractive index contrast  $\Delta$  is 1.9 %, about twice higher than conventional fiber. Smaller outer diameter

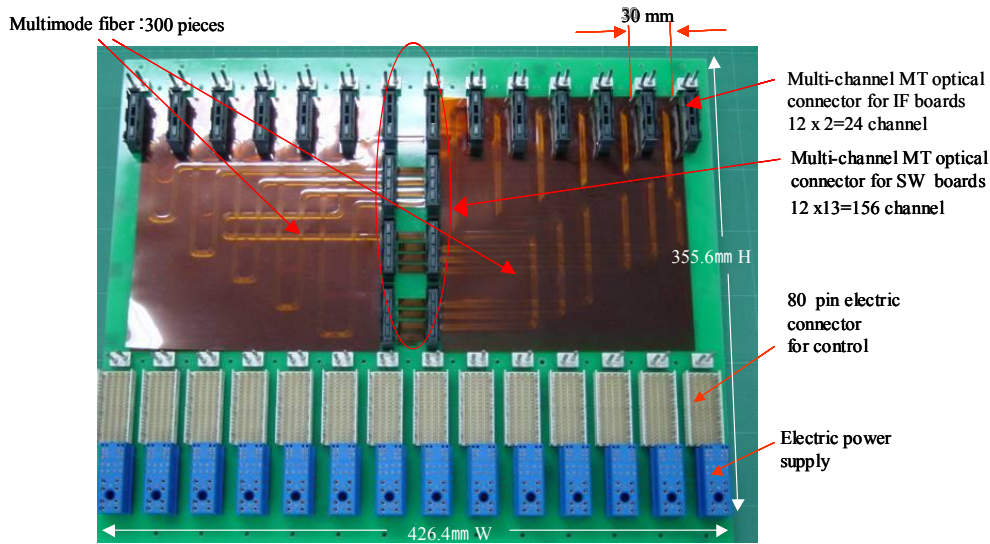


Fig. 2. Photograph of the fabricated backplane

with the conventional 50  $\mu\text{m}$  core leads to reduction of the bending distortion enabling wiring with smaller radius, while maintaining good fiber-to-fiber coupling due to 50  $\mu\text{m}$  core diameter. Higher index contrast enables reduction of the bending loss even in the smaller curvature. Thin resin coating with fiber outer diameter of 125  $\mu\text{m}$  is capable of simple ferrule assembly without removal of the fiber resin coating enabling cost reduction.

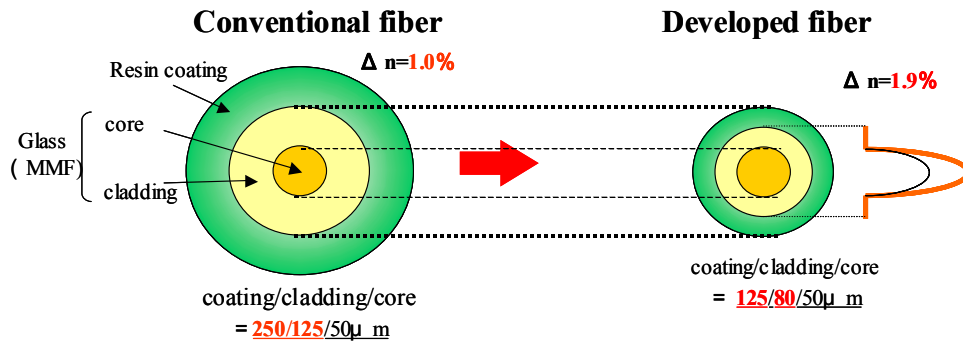


Fig.3. Schematic illustration of the developed fiber with small diameter and high  $\Delta$

As shown in Fig.4, developed fiber exhibits no appreciable bending loss even for the small radius of 5 mm at a wavelength of 850 nm. Figure 5 shows the backplane connector developed compared to the conventional one. Downsizing of the backplane connector has been achieved due to the fiber radius of 5 mm, compared to 20 mm radius of the conventional fiber. Footprint is as small as 6mm x 43 mm. Height is 23 mm. This smaller footprint enables narrower pitch assembly of the optical connector of 20 mm on the fiber board. In the usual MT ferrule assembly, we polish the edge of the fiber after inserting fiber into ferrule. However, when assembling ferrule and fiber board, this usual technique is not adequate. Because the fiber is liable to be broken during polishing, due to shorter fiber leg of the fiber board. Therefore, we have developed new MT ferrule, what we call MTPIPE. The MTPIPE is consisted of the two separated blocks of the rear and front block as shown in Fig.6. Inside the front block, polished fibers are preinstalled. Assembling procedure of the fiber board and ferrule is as follows. First, insert fiber leg part of the board into the rear block and then glue the rear block with the front block having preinstalled polished fibers. Total size of the assembled blocks is the same as the conventional MT ferrule. Figure 7 shows the insertion loss measured for MTPIPE. Insertion loss as low as 0.1 to 0.2 dB was obtained for both angled PC connection and flat PC connections. Also, optical return loss was measured to be as low as -30 to -37 dB for both types of connections, although angled PC connection showed

lower values. These experimental results indicate usefulness of the developed MTPIPE component.

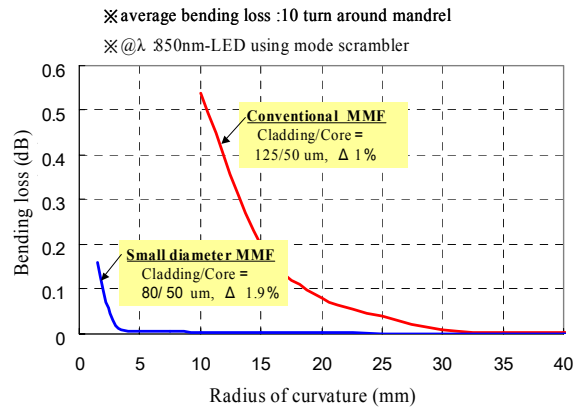


Fig.4. Bending loss of the developed fiber

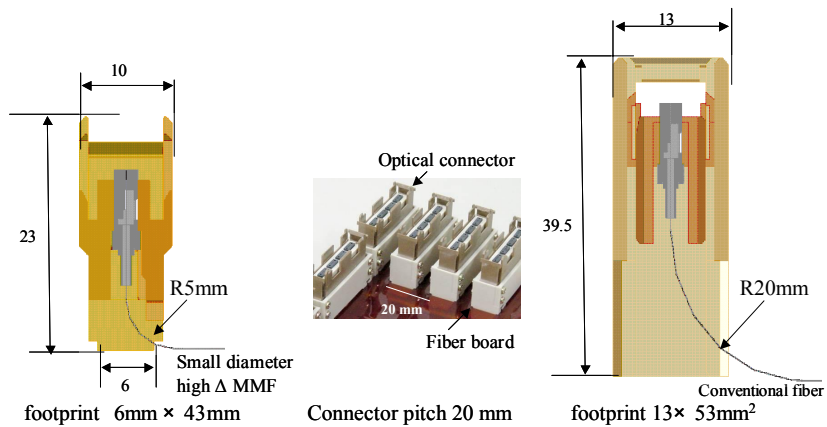


Fig. 5.Backplane connector developed compared to the conventional one

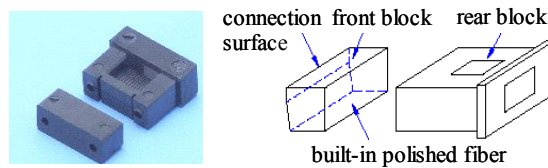
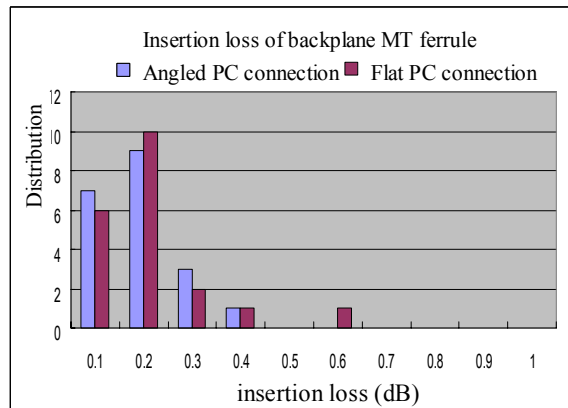
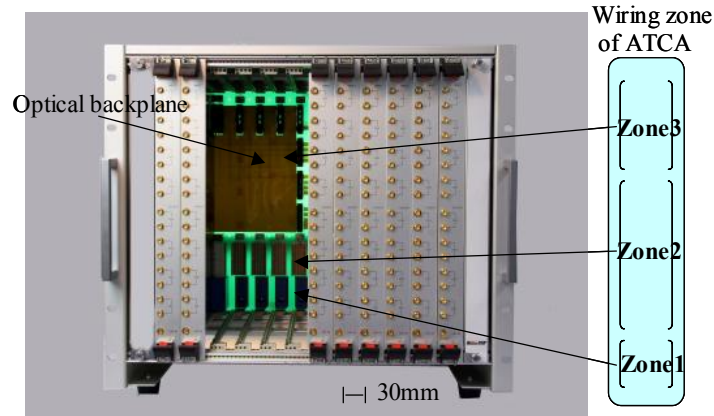


Fig.6. Structure of MTPIPE



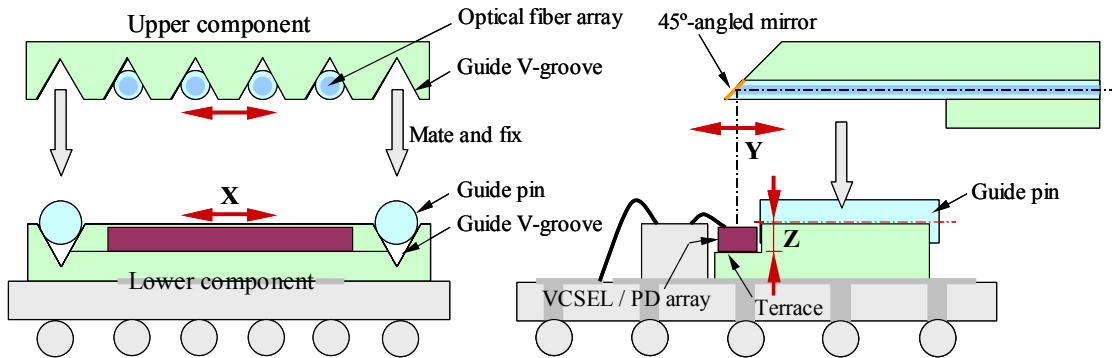
**Fig.7.** Insertion loss measured for MTPIPE

Figure 8 shows 19 inch subrack mounting the optical backplane as a backbone in the upper part of the zone 2 and zone3 of the ATCA standard. Lower part of the zone 2 and zone 1 consists of electrical connectors for controlling signals and power supply.



**Fig.8.** 19 inch subrack mounting the optical backplane

We have developed 4 x 10 Gbps OE/EO optical modules to evaluate the transmission characteristics of the fabricated optical backplane [10],[11]. Schematic cross section of the developed modules is shown in Fig.9. The 4 channel VCSELs or photodiodes are mounted on the terrace of the lower substrate with two fiber guide pins to passively assemble the upper optical I/O component having 4 channel small diameter, high index contrast ( $\Delta$ ) fine multimode fiber which is the same one used to build the backplane aforementioned. These fibers are embedded inside the V-grooves formed at the backside upper component with 45 degree mirror built at the edge of the component for the optical path redirection. Butt-coupling technique without microlens was adopted by carefully designing the z-direction distance from the surface of the OE devices to the center of the upper component fibers to be 45 $\mu$ m. Fairly high coupling efficiency of 70% and large x-y alignment tolerance of +/- 10  $\mu$ m were obtained at the 45  $\mu$ m clearance because of the benefit of the higher  $\Delta$  i.e. larger NA than conventional GI multimode fibers.



**Fig.9.** Schematic cross section of the developed modules

Photographs of the upper and lower components are shown in Fig.10. These components are made of BK-7 glass machined by cutting and grinding for low-cost manufacture. The photograph of the module is shown in Figure 11 with the daughter board where the fabricated OE/EO modules are mounted by BGA connection. The daughter board is 280 mm x 322 mm in size compliant to the ATCA standard specifications. As shown in Fig.12, the board-to-board transmission experiments performed by using the fabricated optical backplane and modules reveal a good eye diagram with a timing margin of 40 ps at 10 Gbps. These transmission experiments indicate 3 Tbps potential of the fabricated backplane with 300 pieces of the high  $\Delta$  fine multimode fibers.

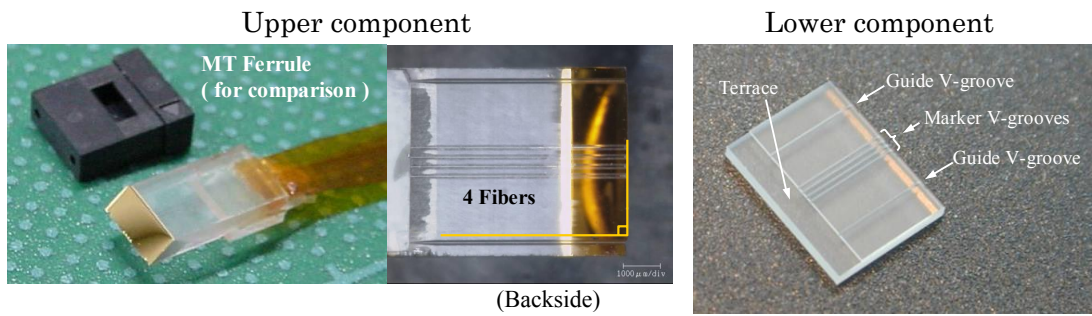


Fig.10. Photographs of the upper and lower components

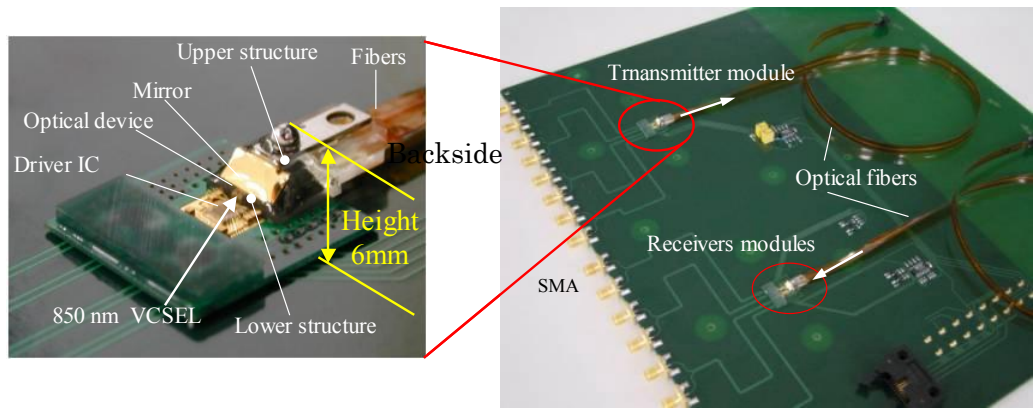


Fig.11. Photograph of the module and module mounted daughter board

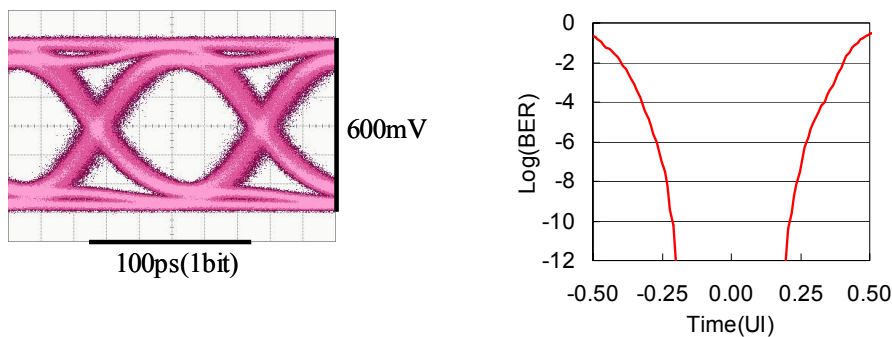


Fig.12. Eye diagram and timing margin measured at 10 Gbps

### 3. OTICAL MODULES

#### 3.1. Low-cost and high-density optical parallel link modules for over 100Gbps applications

To meet high-capacity requirements of high-end routers and servers, development of the OE modules mountable in close proximity to the Switching/CPU LSIs of the inner board area will be crucial to avoid I/O bottleneck of LSI, while maintaining higher data-rate of more than 10Gbps/ch. Figure 13 shows module cost normalized by transmission speed (\$/Gbps) and throughput normalized by module footprint (Gbps/cm<sup>2</sup>) versus various module configurations reported to



date for practical use from long-haul WAN to inter-boxes LAN applications. These kinds of existing modules are applicable to the edge of the daughter boards of the boxes, for example to the interface board edge of the routers to be connected to the outer optical network systems and/or to the multi-cabinet systems of the routers and servers, but are not likely suitable for the inner board applications nearby LSI due to their rather bulky size of these kinds of modules. Furthermore, cost reduction of the modules will be very important because the number of the modules to be placed closely to the LSI will tend to increase with increasing pin count of the high capacity LSIs having large throughput of the order of around 1 Tbps. Therefore, development of the OE modules of high density (Gbps/cm<sup>2</sup>) and low cost (\$/Gbps) will be highly required. To achieve high density, downsizing of the module is indispensable. Also, for cost reduction easy optical coupling between fibers/waveguides and OE devices is crucial to adopt the passive alignment technique, while avoiding optical components such as costly microlens for optical adjustment.

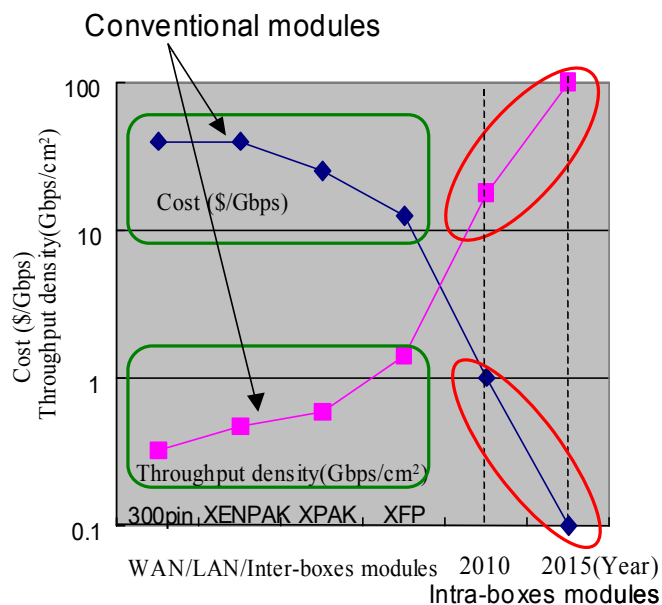


Fig. 13. Module cost (\$/Gbps) and throughput density (Gbps/cm<sup>2</sup>) versus various module configurations

Figure 14 shows schematic cross section and photograph of the developed small form factor 12 channel optical modules for over 100 Gbps inner board applications [17]. The module comprises the pluggable upper block with 12 channel fibers and lower substrate with 12 channel VCSEL or photodiode OE devices and driver/receiver ICs. The module size is as small as 10mm x 10mm in footprint with thickness of 6mm. This module features high transmission density of 120 Gbps/cm<sup>2</sup> in one order of magnitude larger than conventional 10Gbps modules and low-cost structure based on the passively aligned butt-coupling manner without microlens components.

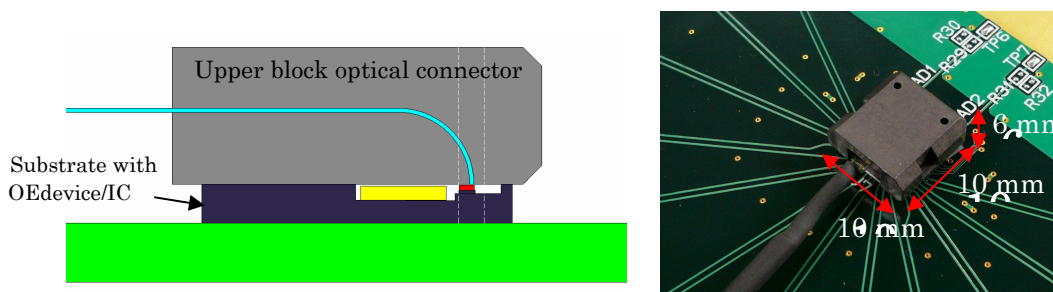


Fig.14. Schematic cross section and photograph of the 12 channel optical modules

As shown in Fig.15, a good eye opening was obtained for 10 Gbps data rate with a received optical power of  $-9.6$  dBm at  $10^{-12}$  BER and at a wavelength of 850 nm.

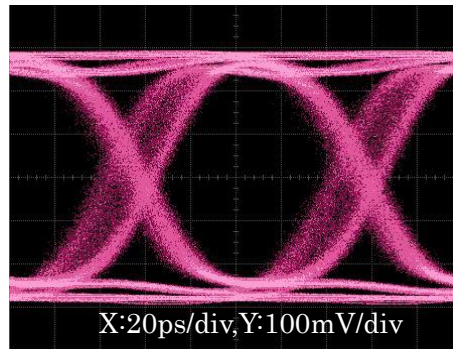


Fig.15. Eye diagram for 10 Gbps at wavelength of 850 nm

The surface mounting technology (SMT) assembling of the optical modules onto the interface board and the photograph of the corresponding OE sub-rack system are shown in Fig.16. Optical module assembling procedure onto the interface

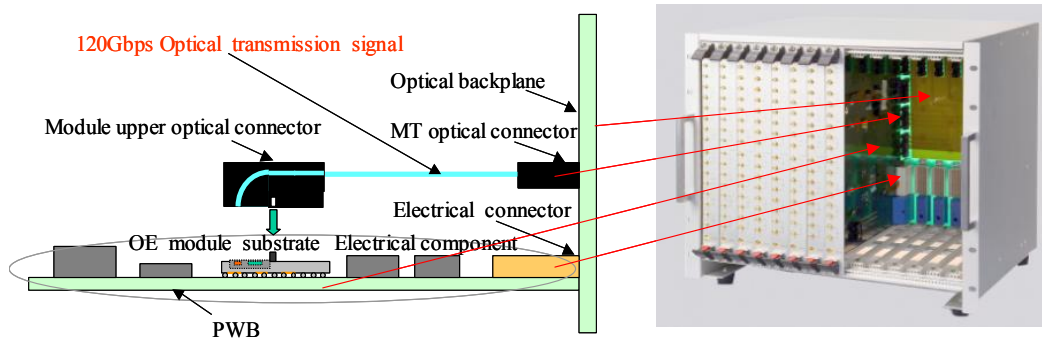


Fig.16. SMT assembling and photograph of OE sub-rack system

board will be as follows: (1)Mounting OE module substrate including OE/EO devices onto the board together with the other electric components, (2)Reflow all of the components on the board, and (3)Mating upper optical connector with OE module substrate. Features of these optical module assembled board will be (1) All surface mounting technology (SMT) for low-cost volume manufacture, (2) Standard electrical PWB technology applicable for interface board and (3) 120Gbps/module high data rate potential. The latter two features lead to easy handling of the board without consciousness of the optics. This unconsciousness of the optics as well as the usability of the conventional SMT technologies will be beneficial to introducing optics inside the boxes due to their low-cost and easy-handling configurations for volume manufacture.

### 3.2. Optical module component technologies for low-cost assembling and high-performances

#### 3.2.1. Monolithic two wavelengths twin VCSELS

In this paragraph, we describe the monolithic two wavelengths twin VCSELS developed for high-density and low-cost packaging [18]. Photograph of the fabricated VCSELS is shown in Fig.17(a). Twin VCSELS having different emitting wavelength of 848 nm and 862 nm are monolithically integrated very closely with each other by varying the thickness of the phase control layer of the cavity. Center-to-center distance of the adjacent mesa of the VCSEL is typically 30  $\mu$ m with the clearance of each mesa of only 5  $\mu$ m. Combination of this closely integrated twin VCSELS and taper waveguide enables densely packaged CWDM configuration as shown in Fig.17(b) by launching the lased beams of each wavelength  $\lambda_1$ ,  $\lambda_2$  simultaneously into the tapered waveguide for wavelength multiplexing. Furthermore, optical coupling between twin VCSELS and waveguide can be achieved without costly micro-optics because of the benefit of the close proximity of each VCSEL and tapered waveguide. The twin VCSELS exhibit a good eye diagram at 13 Gbps, indicating a total of 26 Gbps potential via one channel optical waveguide. The fabricated twin VCSELS will be useful to

manufacture high-density and low-cost optical modules for CWDM applications.

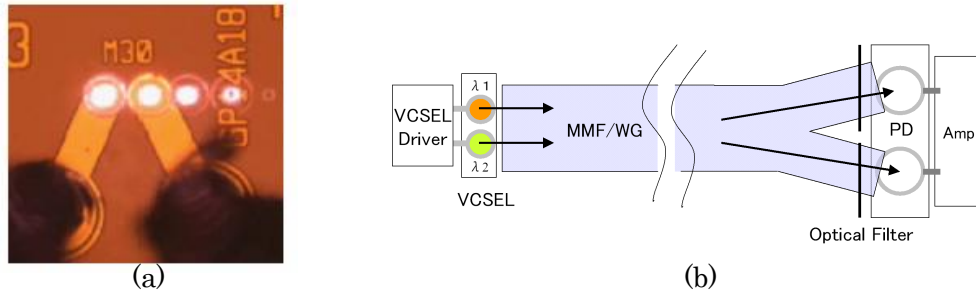


Fig.17. (a)Photograph of monolithic two wavelength VCSEL and (b) densely packaged CWDM configuration

### 3.2.2. Self-alignment optical coupling technology

As described previously, ease of the optical coupling between fibers/waveguides and optical devices is the key issue to be solved to achieve low-cost modules suitable for volume manufacture. Figure 18 shows the process of the self-alignment technique developed for this purpose [19]. In this technique, optical devices can be automatically aligned to the ferruled fiber by the surface tension of the adhesive potted at the edge of the ferruled fiber. Also shown in Fig.18 is the single VCSEL self-aligned to the multimode GI fiber with 50 um core diameter. The VCSEL used in the experiment is the bottom emitting type having anode and cathode electrodes on the opposite side of the emission. The self-aligned VCSEL reveals fairly high-speed operation up to several Gbps. Very low-cost optical modules applicable to the commodity and high-end use will be realized by this developed self-alignment technique.

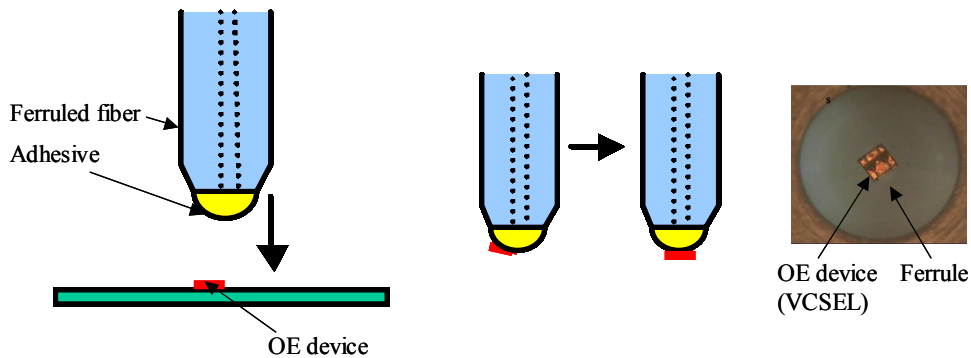


Fig. 18. Process of the self-alignment technique and single VCSEL self-aligned to the ferruled fiber

## 4. CONCLUSIONS

Solutions ranging from the optical backplane platform to the module component technologies have been discussed. These technologies include the Advanced-TCA standardized optical backplane for practical use and the low-cost and high-density optical parallel link modules to be assembled onto the board for over 100Gbps applications. Optical module component technologies such as the monolithic two wavelengths twin VCSELs based on the CWDM approach and the self-alignment technique of easy optical coupling have been demonstrated for low-cost and high-density packaging. These technologies will be useful to alleviate difficulties of optics penetration inside the boxes.

## REFERENCES

- [1]Optoelectronic Industry and Technology Development Association(OITDA) report, p.30,2006(in Japanese).
- [2]Rich Warmke,“Rambus Memory Interface Technology,” RAMBUS DEVELOPER FORUM JAPAN, July, 2005.
- [3]Alexei L.Glebov, M.G.Lee,K.Yokouchi, ”Integration technologies for pluggable backplane optical interconnect systems,” Optical Engineering 46(1),p.015403-1,2007.
- [4]E.Bosman,G.Van Steenberge,P.Geerinck,W.Christiaens,J.Vanfleteren and P.Van Daele, ”Embedding of Optical

- Interconnections in Flexible Electronics,” Proc. of 57th ECTC, p.1281, 2007.
- [5] B.J. Offrein, C. Berger, R. Beyeler, R. Dangel, L. Dellmann, F. Horst, T. Lamprecht, N. Meier, J. Kash, “High bandwidth board-level parallel optical interconnects for server applications,” Proc. of 32th ECOC, We4.2.1, 2006.
- [6] D. Guidotti, J. Yu, M. Blaser, V. Grundlehner and G.K. Chang, “Edge Viewing Photodetectors for Strictly In-plane Lightwave Circuit Integration and Flexible Optical Interconnects,” Proc. of 56th ECTC, p.782, 2006.
- [7] R.T. Chen, J. Choi, L. Wang, H. Bi, “Recent Advances of Chip-to-Chip Optical Interconnect Systems,” 16th LEOS HSD Workshop Notes, TuB4, 2005.
- [8] <http://io.intec.ugent.be/publications.html>, “Parallel optical interconnects with on-chip optical access,” SPIE Photonics Europe, 2004.
- [9] M.A. Shahid and W.R. Holland, “Flexible Optical Backplane Interconnections,” Proc. of MPPOI, p.178, 1996.
- [10] A. SUZUKI, K. SUZUKI, Y. WAKAZONO, S. SUZUKI, T. YAMAGUCHI, H. MASUDA, K. SAITO, M. KINOSHITA, O. IBARAGI, K. KIKUCHI, H. NAKAGAWA, Y. OKADA, and M. AOYAGI, “Signal Transmission Evaluation of Optical Backplane Model with 10-Gbit/s Optical Transmitter and Receiver Module,” IEICE, Vol. J89-C, p. 796, 2006 (in Japanese).
- [11] A. Suzuki, K. Suzuki, Y. Wakazono, S. Suzuki, T. Yamaguchi, H. Masuda, K. Saito, M. Kinoshita, O. Ibaragi, K. Kikuchi, H. Nakagawa, Y. Okada, and M. Aoyagi, “Low-cost and high-density 10Gbps/ch optical parallel link module for multi-terabit router application,” Proc. of 32th ECOC, We.4.2.3, 2006.
- [12] V. Sharma, “Advanced Telecommunications Computing Architecture and micro TCA Next Generation Standards based Network Equipment High Speed Interconnect,” 16th LEOS HSD Workshop Notes, TuA4, 2005.
- [13] I. Hatakeyama, K. Miyoshi, J. Sasaki, K. Yamamoto, M. Kurihara, T. Watanabe, J. Ushioda, Y. Hashimoto, R. Kuribayashi, and K. Kurata, “A 400 Gbps Backplane Switch with 10 Gbps/port Optical I/O Interfaces,” Proc. of the SPIE, Vol. 6014, 158, 2005.
- [14] D.M. Kuchta, Y.H. Kwark, C. Schuster, C. Baks, C. Haymes, J. Schaub, P. Pepeljugoski, L. Shan, R. John, D. Kucharski, D. Rogers, M. Ritter, J. Jewell, L.A. Graham, K. Schroedinger, A. Schild and Hans-Martin Rein, “120-Gb/s VCSEL-Based Parallel-Optical Interconnect and Custom 120-Gb/s Testing Station,” IEEE J. Lightwave Tech. 22, p.2200, 2004.
- [15] <http://www.ieee802.org/3/hssg/index.html>.
- [16] P. K. Pepeljugoski, “Emerging 100GE Standards and Challenges,” 18th LEOS HSD Workshop Notes, MA1, 2007.
- [17] to be presented in SPIE Photonics West 2008.
- [18] T. Suzuki, Y. Wakazono, A. Suzuki, T. Ishikawa, H. Masuda, Y. Hashimoto, K. Kikuchi, M. Tamura, H. Nakagawa, M. Aoyagi, and T. Mikawa, “13Gbps Multi Wavelength CWDM Monolithic VCSELs for High Density Packaging,” Proc. of 13th MOC, PD2, 2007.
- [19] to be published in IEEE Photonics Technology Letters.
- [20] Optoelectronic Industry and Technology Development Association (OITDA) report, 2004FY-009-1, p.5, 2005 (in Japanese).

## Fully Embedded Board Level Optical Interconnects—From Point-to-Point Interconnection to Optical Bus Architecture

Xiaolong Wang

Omega Optics Inc., Austin, TX, 78758

Ray T.Chen

University of Texas at Austin, Austin, TX, 78758

**Abstract:** This paper presents the latest progress toward fully embedded board level optical interconnects in the aspect of optical bus architecture design, waveguide fabrication and device integration. A bidirectional optical bus architecture is designed and can be fabricated by a one-step pattern transfer method, which can form a large cross section multimode waveguide array with 45° micro-mirrors by silicon hard molding method. The waveguide propagation loss is reduced to 0.09dB/cm and the coupling efficiency of the metal-coated reflecting mirror is experimentally measured to be 85%. The active optoelectronic devices, vertical surface emitter lasers and p-i-n photodiodes, are integrated with the mirror-ended waveguide array, and successfully demonstrate a 10 Gbps signal transmission over the embeddable optical layer.

**Key words:** optical interconnects; optical bus; 45° micro-mirrors; hard molding; polymer waveguide; optical printed circuit board

### I. Introduction

The speed and complexity of integrated circuits are increasing rapidly as integrated circuit technology advances from very-large-scale integrated (VLSI) circuits to ultra-large-scale integrated (ULSI) circuits. The number of devices per chip, the number of chips per board, the modulation speed, and the degree of integration continue to increase. The International Technology Roadmap for Semiconductors (ITRS) expects that on-chip local clock speed will constantly increase to 10 GHz by the year 2011[1]. The backplane frequency will boost proportionally to meet the interconnection requirement. The third-generation I/O protocol called peripheral component interconnect (PCI) Express, developed by the Signal Interest Group (SIG) consortium, is becoming an industry standard [2]. PCI Express is expected to increase transfer rates up to 10GHz in the next 7-10 years. Beyond 10GHz, copper interconnects on PCB made of FR4 material, become bandwidth limited due to losses such as the skin effect in the conductors and the dielectric loss from the substrate material. It has been reported that replacing the flame resistant 4 (FR4) material with newer laminates such as Rogers 4000 can extend the bandwidth of electrical interconnects to 7.7GHz, but increase the cost by five times [3]. Besides the cost issue, several much worse situations for electrical interconnects are introduced by the unsolvable frequency dependent loss, reflection and cross talk.

Optical solutions, which are widely agreed as a better alternative to upgrade the system performance, have been proposed for the upcoming electrical interconnect bottleneck for over 20 years [4]. Optical interconnects preponderate over the copper links in immunity to electromagnetic interference,

independency to impedance mismatch, less power consumption, and high speed operation. Many optical interconnects schemes have been proposed and investigated, including free space [5], embedded fiber connection [6] and optical slots [7]. However, most of them can only provide a unidirectional point-to-point interconnection. Additionally, these optical interconnects implementations lack a seamless interface with electrical components from the system packaging point of view. For example, the board level optical interconnections reported in [5] piled up lasers, detectors and micro-lens on the surface of a printed circuit board (PCB). The difficulties regarding packaging, multilayer technology, and reliability still remain to be solved.

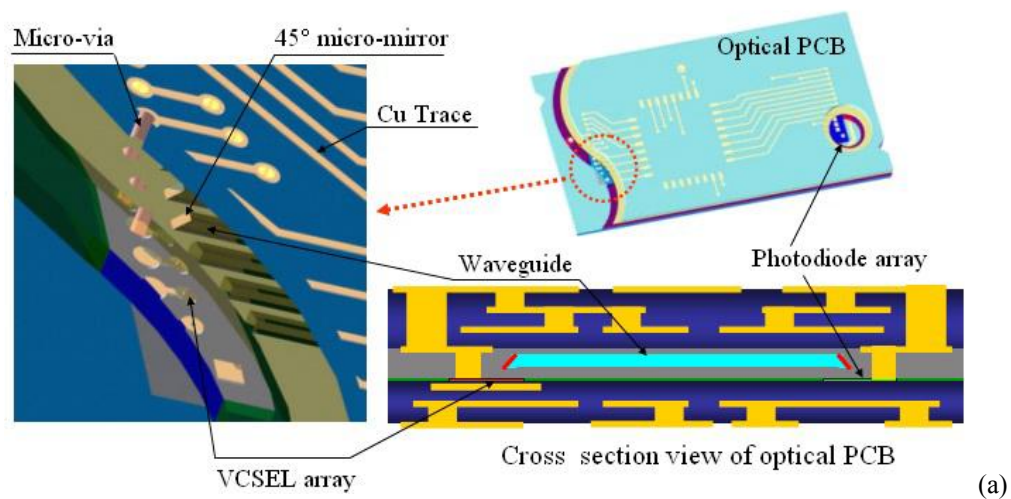
We previously introduced a fully embedded board-level optical interconnects to relieve the packaging difficulty [8]. And later on, another paper was published to describe the fabrication of flexible optical waveguides, thermal management of embedded thin-film vertical surface emitter lasers (VCSELs), and optical layer integration with VCSELs and photodiode arrays [9]. In this paper, the latest progress to fulfill the fully embedded optical interconnects with optical bus architecture is presented. An improved fabrication procedure of a large cross section multimode waveguide array with 45° micro-mirrors by one-step pattern transfer method is presented. Low propagation loss waveguides as well as high coupling efficiency micro-mirrors are experimentally obtained and measured, using a new fabrication process in contrast to Ref. 9. The active optoelectronic devices, VCSELs and p-i-n photodiodes, are integrated with the mirror-ended waveguide array, and successfully demonstrate a 10Gbps signal transmission over the embeddable optical layer for the first time.

## **II. Fully Embedded Board Level Optical Interconnects based on Optical Bus Architecture**

For electrical interconnects, the point-to-point topology has replaced the shared-bus topology because of its bandwidth. However, wiring congestion is the adverse consequence of this transition, because in order to route all memory modules to the central switch, the boards in a high performance computing system currently tend to use more than 50 wiring layers, and more than 700 signal pins are required for one board edge connector, which needs as large as 100 pounds insertion force to seat [10]. Optical bus architecture [11-12] greatly mitigates the wiring congestions, while still allows multiple daughter boards to share a common data channel to transfer information at a high speed simultaneously. There is no loading effect of optics analog to driving capacitance in electronic circuit, which means the signal propagation speed is a constant value of 0.6c of polymer waveguide regardless of the presence of the receiver boards. While for electrical bus, an unloaded PC board trace has a typical signal propagation speed of 0.6c to a fully loaded bus line of 0.2c. Higher speed as well as a much more stable signal round-trip time can be obtained by replacing the electrical bus with the proposed optical bus. Comparing with point to point interconnect, bus based interconnects represent the most complicated interconnect structure with full interconnectivity and broadcasting nature. Fiber based optical interconnects, which is intrinsically for point-to-point interconnection, fails to provide the desired optical bus architecture. As a comparison, polymer waveguides can be easily manipulated to form a complicate interconnection structure that is indispensable for a bi-directional optical bus [8,13].

The architecture of the fully embedded optical layer includes a VCSEL array, a p-i-n photodiode array,

surface-normal micro-mirrors, and a polymeric channel waveguide array with 45° micro-mirrors functioning as a physical layer of optical interconnection. The driving electrical signals to modulate the VCSELs and the demodulated signals received at the photodiode flow through electrical vias connecting to the surface of the PC board, as seen in Fig.1 (a). Within the optical interconnect layer, the light from the VCSELs is coupled into/out of the waveguide through 45° micro-mirror couplers and propagates in the polymer waveguide. The fully embedded structure makes the insertion of optoelectronic components into microelectronic systems much more realistic when considering the fact that the major stumbling block for implementing optical interconnection onto high-performance microelectronics is the packaging incompatibility. Fig.1 (b) shows the in plan view of the optical equivalent of a single bidirectional electronic bus line. The optical waveguide plane consists of two parallel optical buses, which can transmit optical signals toward two opposite directions. Optical signals, either from laser diodes (LD) of the master unit or the slave units, will be transmitted bidirectionally through two connected unidirectional couplers. The detectors (D) of either the master unit or the slave units are capable of receiving optical signals from both directions also, benefited from the two unidirectional couplers connected to them. The two parallel optical buses in conjunction with unidirectional couplers ensure the completely non-blocking interconnection among any existing units, without any wiring congestions. The laser diodes and photodetectors belong to another plane. The drive current provided by each electronic transceiver powers the corresponding laser diode, whose output is split and injected into both unidirectional couplers. Each photodiode detects light from either unidirectional coupler, whose current powers the corresponding electronic receiver. The laser diodes and the photodetectors are located either on the associated cardboards or the backplane itself. The intra-plane interconnection, i.e., from the laser diodes and photodetectors to the waveguides, are established through surface normal micro-mirrors.



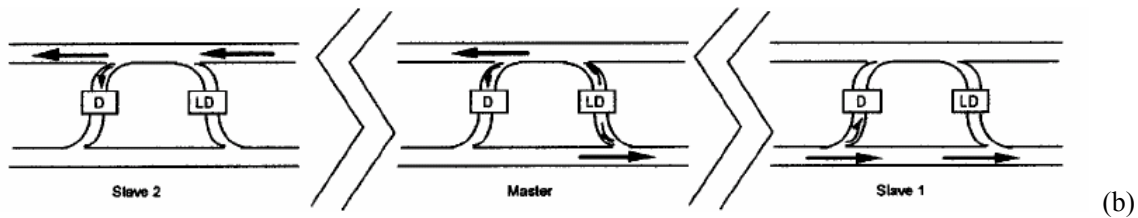


Fig 1 (a) Fully embedded board level optical interconnects architecture (b) In plane view of the optical equivalent of a bidirectional electronic bus line driven by open-collector drivers (D: detector, LD: laser diode, coupling to the in plane waveguide through 45° mirror)

The optical waves can be either coupled into and out of the optical bus by two opposite-placed 45° micro-mirrors, as Fig. 2 (a) shows, or by one micro-mirror and equally split by a Y-branch coupler, as Fig 2 (b) shows. The fabrication process for the bidirectional bus structure is completely compatible with that for the parallel point-to-point optical interconnects.

To fulfill the embedded structure, two major stumbling blocks need to be solved. A low cost, high performance optical layer on a polymer thin film represents the first. Packaging the optical layer through via holes and laminating it inside PCB layers stands for the second. The research work presented herein will relieve the concerns for the first major block, and is believed to be able to accelerate the deployment of the fully embedded optical interconnect architecture.

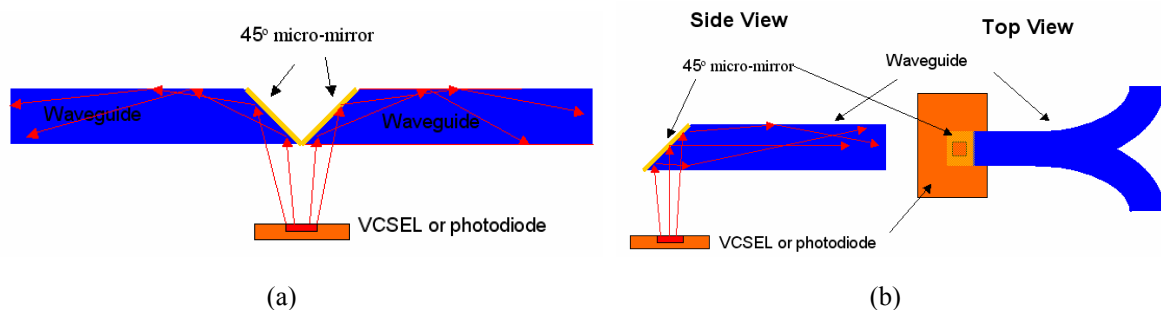


Fig 2 3D bidirectional intra-plane couplings through (a) two opposite placed 45° micro-mirrors and (b) one 45° micro-mirror and one Y-branch coupler

### III. Fabrication of Waveguide Array with Micro-Mirrors

We previously demonstrated a soft-molded waveguide layer with 45° coupling mirrors that is suitable for the embedded structure [14]. Soft molding method utilizes properly shaped flexible molds—often made of elastomeric polydimethylsiloxane (PDMS) for pattern transfer. Although cheap and easy for fabrication, soft molding method still faces serious problems such as durability and size precision. Due to its low Young’s module, the soft mold will deform even under a small pressure, resulting in a reduced channel depth and enlarged pitch distance. This expanded pitch will cause the waveguide alignment difficulty with the VCSELs and photodiode array resulting in increased coupling loss. These shortages can be overcome by replacing the soft mold material with silicon based hard mold.



Although the silicon master mold, fabricated by photolithography and deep reactive ion etching (DRIE) method, is more expensive than the PDMS soft mold, the production cost per waveguide array is still cheaper than soft-molding method when considering its long durability.

A hard molding fabrication process using UV embossing method is conducted on a 100 $\mu\text{m}$  thick topas film. The topas film is chosen because of its transparency and high glass transition temperature ( $T_g > 160^\circ\text{C}$ ) [9]. The main procedure is divided as the following steps shown in Fig.3:

(a) First, a layer of UV curable bottom cladding material, WIR30-450 (from ChemOptics, with a refractive index of 1.45 at 850nm wavelength) is spin coated on the topas film substrate.

(b) In the second step, the master mold is brought in contact with the spin-coated substrate, and the molded WIR30-450 layer is UV cured for 8 minutes inside a nitrogen atmosphere.

(c) To separate the polymer substrate with the silicon master mold, the sample is immersed in acetone to quickly dissolve the photoresist layer on top of the silicon pattern. The intact polymer substrate will detach the master mold within 1 minute. After forming the desired trenches, a core material WIR30-470 with a higher refractive index (1.47 at 850nm) is used to fill them up. The excess polymer is scraped off, and the same amount of UV dose is applied to cure the core layer.

(d) In the last step, the sample is spin coated with another layer of WIR30-450, which functions as the top cladding, and followed by a UV curing process.

Unlike hot embossing [15] or PDMS soft-molding [9] methods, there are no fabrication steps associated with high pressure or heating. This ensures the replicated waveguide array to have an exact size as the original silicon master mold, and thereby reduces the fabrication cost and energy consumption. The propagation loss of the waveguide is measured by the cutback method. An 850 nm VCSEL light is coupled into the waveguide by a 50/125 $\mu\text{m}$  graded index multimode fiber and the output beam is then coupled into a photodetector by a 62.5/125 $\mu\text{m}$  graded index multimode fiber. The measured propagation loss is 0.09dB/cm at 850 nm. This data is close to the planar waveguide loss of 0.05dB/cm provided by the material vendor.

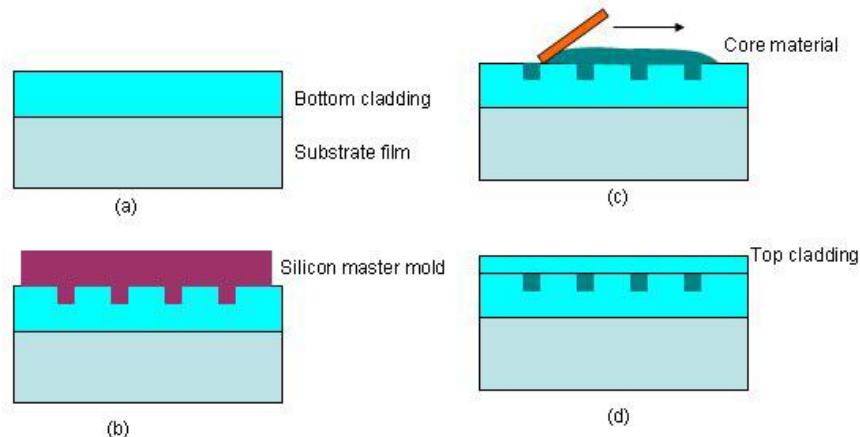


Fig.3 UV embossed molding process of the polymer waveguide array

Waveguide couplers play a key role for the realization of three-dimensional fully embedded board-level optical interconnection owing to their surface-normal coupling of optical signals into and

out of in-plane waveguides. A waveguide grating [8] as well as a 45° waveguide mirror based coupler [14] can serve as a surface normal coupler. However, the grating based approach requires precise control of grating parameters for efficient coupling and usually has a low tolerance to wavelength variations. Therefore, we employ 45° total internal reflection (TIR) coupling mirrors at both ends of waveguides because they are easy to fabricate, reproducible, and relatively insensitive to wavelength variations, and can provide a high coupling efficiency.

The waveguide micro-mirror can be fabricated by a one-step pattern transfer method described in [14]. After the DRIE process, the silicon master mold is mechanically polished on both ends using a specially designed 45° stage. The polishing process starts from a 30μm grits lapping pad to 1μm grits. Finer polishing is unnecessary since the following spin-coated surface treating process will smear the remained roughness. The 45° tilted end surfaces will be transferred to the UV cross linked polymer substrate that is in direct contact with the master mold. The waveguide array pattern, together with the desired micro-mirror coupler, is replicated in a negative shape from the master structure simultaneously. To further reduce the fabrication effort described in [14] using standard photolithography and followed by lift-off process, the sample is covered by a polymer thin-film mask with opened mirror windows. This reusable thin film mask will shield the deposition of metal layer on the polymer substrate except in the open windows. An electron beam evaporated 200nm thick gold layer is deposited to form the high reflectivity mirrors. After removing the thin film mask, the UV embossed trenches with metal mirrors on both ends, can be filled with the core material.

The SEM image of the polished surface on the silicon master mold is shown in Fig.4 (a). To observe the light transmission over the UV embossed waveguide array with the embedded 45° micro-mirrors, a 9μm core diameter fiber coupled with a 633nm He-Ne laser vertically launch the input light into the waveguide mirrors. The input fiber is purposely pulled 5mm above the mirror surface to co-illuminate the 1X12 mirror array. At the back end, the output field patterns are projected onto an image scope, which can be viewed through a monitoring screen. The output pattern of the twelve reflecting mirrors is shown in Fig.4 (b). We measured the total insertion loss of the twelve channels at 850nm wavelength. By comparing the results with the values for straight waveguides of the same length and dimension, we extracted the total coupling loss of the front and back mirrors. Assuming the two mirrors have the same coupling efficiency, which is approximately correct, the obtained coupling loss is 0.7~1.5dB for each mirror. In another word, the highest coupling efficiency is 85%.

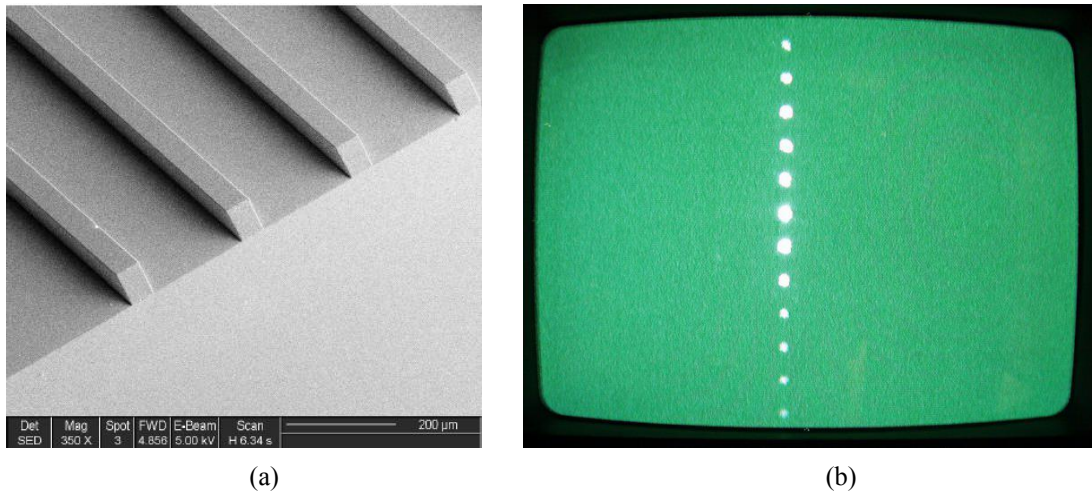


Fig.4. Experimental results of the micro-mirror array (a) SEM image of the silicon master mold with polished surface (b) output pattern from the image screen

#### IV. Prototype system demonstration

Figure.5 shows the testing setup for the prototype optical layer, which is embeddable to the PC boards, with an enlarged view of the microwave probes approached to the integrated photodiode array.

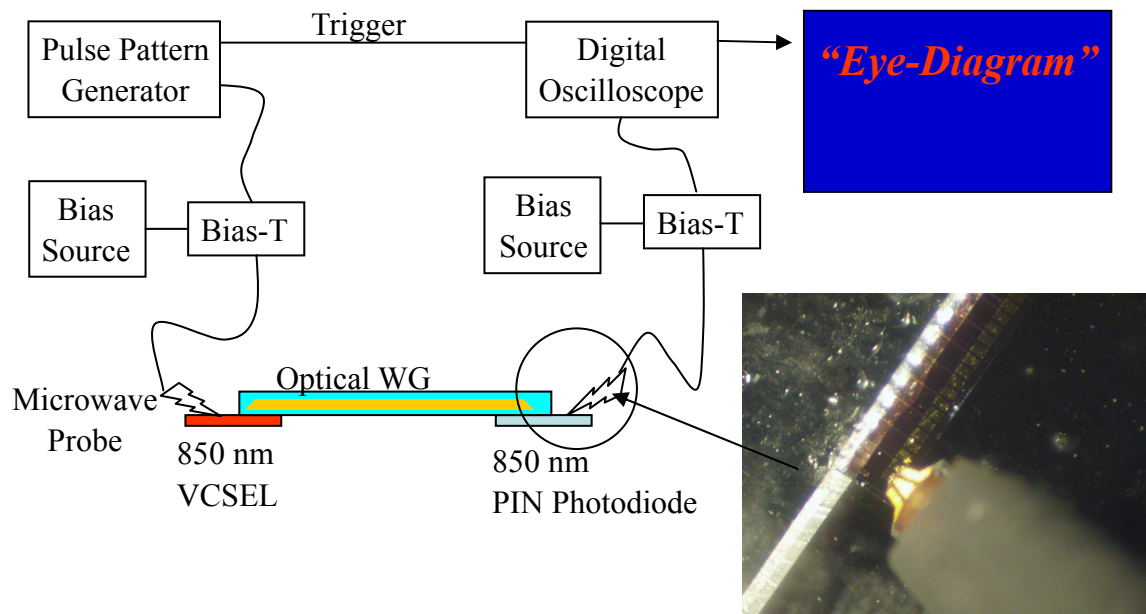


Fig.5 Schematic diagram of the measurement setup for the assembled optical system

The VCSEL is biased with a lasing current, and the photo current from the p-i-n diode is measured as well. The maximum response from the photodiode is  $300\mu\text{A}$ . The VCSEL is then biased at  $5\text{mA}$  and modulated by a  $\pm 0.3\text{V}$   $10\text{ Gbps}$  pseudo random signal. The response from the photodiode is directly connected to a digital oscilloscope without any pre-amplification. The measured eyediagram is shown in Fig.6, with a Q-factor of  $7.24$ , corresponding to a bit error rate (BER) below  $10^{-12}$ .

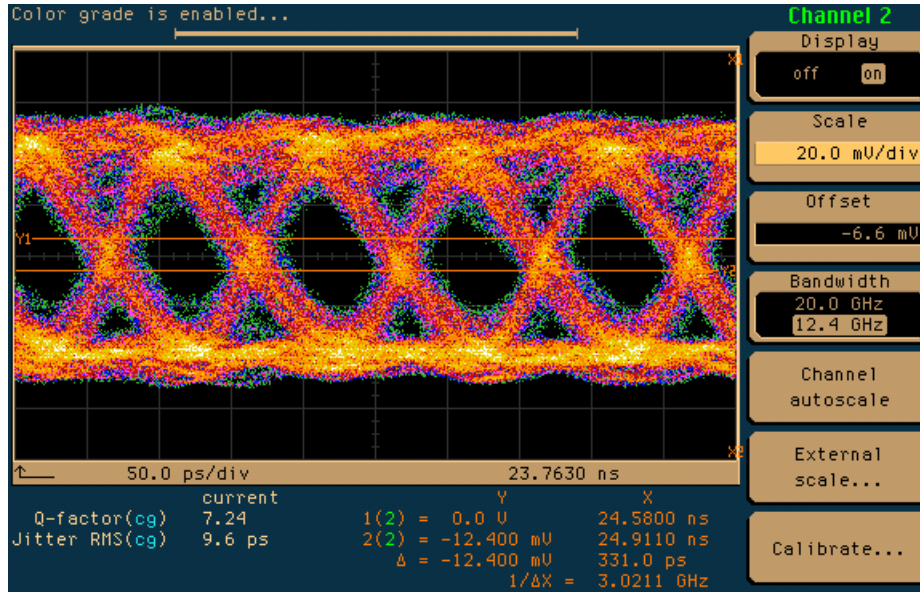


Fig.6 Measured 10Gbps eyediagram with a Q-factor of 7.24

## V. Conclusion

This paper presented the latest progress of device fabrication and system integration for fully embedded board level optical interconnects based on optical bus architecture. Further investigation including metal plate molding process, bi-directional bus structure, and integration with printed circuit boards will be conducted.

Acknowledgement: The work is sponsored by National Science Foundation (NSF).

## Reference

- [1] International SEMATECH, "The National Technology Roadmap for Semiconductors (ITRS)—Technology Needs," Semiconductor Industry Association, 2005.
- [2] S. Berry, "Advanced Bus and Interface Market and Trends," *Electronic Trend Publication Inc.*, September 2003.
- [3] D. Huang, T. Sze, A. Landin, R. Lytel, and H. L. Davidson, "Optical interconnects: Out of the box forever?" *IEEE J. Sel. Top. Quan. Elec.*, vol. 9, no. 2, pp. 614-623, 2003.
- [4] J. W. Goodman, F. I. Leonberger, S. Y. Kung, and R. A. Athale, "Optical Interconnections for VLSI Systems," *Proc. IEEE*, vol. 72, no. 7, pp. 850-866, 1984.
- [5] E. M. Strzelecka, D. A. Loudereback, B. J. Thibeault, G. B. Thompson, K. Bertilsson, and L. A. Coldren, "Parallel free-space optical interconnect based on arrays of vertical-cavity lasers and detectors with monolithic microlenses," *Appl. Opt.*, vol. 37, no.14, pp.2811-2821, 1998
- [6] M. Schneider, T. Kühner, "Optical interconnects on printed circuit boards using embedded optical fibers," *Proc. Of SPIE*, vol.6185, 61850L-1, 2006
- [7] I. K. Cho, K. B. Yoon, S. H. Ahn, and H. K. Sung, "Experimental demonstration of 10Gbit/s transmission

- with an optical backplane system using optical slots,” *Opt. Lett.*, vol.30, no.13, pp.1635-1637, 2005
- [8] R. T. Chen, L. Lin, C. Choi, Y. Liu, B. Bihari, L. Wu, S. Tang, R. Wickman, B. Picor, M. K. Hibbs-brenner, J. Bristow, and Y. S. Liu, “Fully Embedded Board-Level Guided Wave Optoelectronic Interconnects,” *Proc. Of the IEEE*, vol.88, no.6, pp.780-794, 2000
- [9] C. Choi, L. Lin, Y. Liu, J. Choi, L. Wang, D. Haas, J. Magera, R. T. Chen, “Flexible optical waveguide film fabrications and optoelectronic devices integration for fully embedded board-level optical interconnects ,” *IEEE J. of Lightwave Technol.*, vol. 22, no.9, pp.2168 – 2176, 2004
- [10] D. Huang, T. Sze, A. Landin, R. Lytel, and H. L. Davidson, “Optical interconnects: out of the box forever?” *IEEE Journal of Selected Topics in Quantum Electronics*, vol. 9, No.2, pp.614-624 (2003)
- [11] X., Han, G. Kim, G. J. Lipovski, and R. T. Chen, “An optical centralized shared-bus architecture demonstrator for microprocessor-to-memory interconnects,” *IEEE J. Sel. Topics Quantum Electron.*, vol.9, no. 2, pp. 512–512 (2003)
- [12] H. Bi, X. Han, X. Chen, W. Jiang, J. Choi, and R. T. Chen, “15Gbps Bit-Interleaved Optical Backplane Bus using Volume Photo-polymer Holograms,” *IEEE Photonics Technology Letters*, Vol.18, pp.2165-2167 (2006)
- [13] R. T. Chen, “VME Optical Backplane Bus for High Performance Computer,” *Optoelectronics-Devices and Technologies*, Vol.9, No.1, pp.81-94 (1994)
- [14] L. Wang, X. Wang, W. Jiang, J. Choi, H. Bi, and R. T. Chen, “45° polymer-based total internal reflection coupling mirrors for fully embedded intraboard guided wave optical interconnects,” *Appl. Phys. Lett.*, vol.87, no.14, 141110, 2005
- [15] K. B. Yoon, C. G. Choi, S. P. Han, “Fabrication of multimode polymeric waveguides by hot embossing lithography,” *Jap.J.of Appl. Phys.*, vol.43, no.6A, pp.3450-3451, 2004



# Towards Flexible Routing Schemes for Polymer Optical Interconnections on Printed Circuit Boards

N. Hendrickx<sup>\*a</sup>, G. Van Steenberge<sup>a</sup>, E. Bosman<sup>a</sup>, J. Van Erps<sup>b</sup>, H. Thienpont<sup>b</sup>, P. Van Daele<sup>a</sup>  
<sup>a</sup>Ghent University, Dept. of Inform. Technology, Technologiepark 914A, B-9052 Ghent, Belgium;  
<sup>b</sup>Vrije Universiteit Brussel, Dept. of Applied Physics and Photonics, Pleinlaan 1, B-1050 Brussels, Belgium

## ABSTRACT

Multilayer optical interconnects offer high interconnection densities and flexible routing schemes. Signals can be routed between the different layers, which can limit the number of cross-overs. In addition, the characteristics of 2D optoelectronic elements can be fully exploited. The alignment between the different optical elements is critical for the performance of the system. Efficient coupling structures are required to couple the light signals between two layers. We propose the use of laser ablated 45° mirrors, which are integrated with the waveguides. Two mirror configurations are proposed: one based on total internal reflection (TIR) and a metallized 45° mirror. A two layer optical structure is presented that contains multimode waveguides and micro-mirrors. The achievable alignment accuracy between the multimode waveguides and micro-mirrors in the two layers is in accordance with the results obtained from a numerical study. Experimental realizations of the mentioned structures and the first results on the loss measurements on the mirrors are presented.

**Keywords:** Laser ablation, optical interconnections, polymer waveguides, coupling structures, printed circuit board, multilayer structures

## 1. INTRODUCTION

Optical interconnections offer a possible solution to the bandwidth problems that are associated with electrical interconnects. The introduction of optical interconnections to the board level has been proposed for high-performance applications where high speed and interconnection densities are an issue. The main reason is the fact that optical interconnections offer an inherently high bandwidth and do not suffer from frequency-dependent loss and electromagnetic interference/compatibility problems as opposed to electrical interconnections where these problems lead to a significant bandwidth limitation at high frequencies<sup>1</sup>. The use of a hybrid electro-optical board, which contains optical interconnections for the high-speed/bandwidth data transfer and electrical interconnects for the remaining interconnects, could overcome this problem<sup>2</sup>. The integration of the optical interconnections to the board-level can be done with the use of a polymer optical layer, which contains multimode optical waveguides and other passive optical elements and which can be laminated inside the board or put on top of the board. The optical layer consists of a cladding-core-cladding stack and can be applied onto the board with a variety of technologies such as spin coating. The used polymer materials must show excellent optical and thermal properties and have to withstand the high temperatures and pressures that occur during standard Printed Circuit Board (PCB) manufacturing and soldering processes. The technology that is used for the micro-structuring technology of the optical layer also has to be compatible with the standard PCB manufacturing and soldering processes. This requirement needs to be fulfilled in order to come to a cost-effective solution that can be adopted by the industry on a reasonable timescale.

The interest in multilayer optical structures, which consist of a stack of optical layers, is growing, in view of its ability to increase the integration density. In addition, the routing of the optical signals can be simplified, making full use of the 2-D characteristics of 2-D optoelectronic elements such as vertical-cavity surface-emitting laser and photodetector arrays.

\*[nina.hendrickx@intec.ugent.be](mailto:nina.hendrickx@intec.ugent.be); phone +3292645370 ; fax +3292645374

It is believed that two optical layers will be sufficient in fulfilling the upcoming demands concerning bandwidth and transfer speed<sup>3</sup>. It should however be noted that the complexity of the structure increases with each additional optical layer. We present laser ablation as an alternative micro-structuring technology that can be used for the structuring of the functional elements of an optical interconnection into a polymer optical layer.

## 2. LASER ABLATION

Laser ablation is a flexible non-contact micro-structuring technology that can be used to pattern a large variety of materials, depending on the used laser source. The patterning relies on the controlled removal of material. The photon energy of the laser beam is used to decompose the material through photo-chemical and photo-thermal processes. The technology is fully compatible with standard PCB manufacturing and is already used for the laser-drilling of micro-vias in high density and high performance electrical boards. Polymer materials typically show a high absorption in the UV-region which makes them a good candidate for ablation with UV-lasers. A clean ablation with low deposition of debris can be obtained in the case that the polymer material efficiently absorbs the emitted laser wavelength.

The available ablation set-up contains three different laser sources: KrF excimer laser (248nm), frequency tripled Nd-YAG (355nm) and CO<sub>2</sub> (9.6µm) laser<sup>4</sup>. This allows us to pattern a large variety of materials. A KrF excimer laser (248 nm) is used for the patterning of multimode waveguides, micro-mirrors and alignment features. A picture and scheme of the excimer laser setup is shown in Fig. 1. During the processing the sample is placed on a computer-controlled translation stage with an accuracy of 1µm. The laser beam is sent through an aperture and projected onto the sample with a demagnification of ten. The dimensions of the ablated structures can be changed in a very flexible way by using the appropriate aperture. The laser beam can be tilted with respect to the sample, which eases the structuring of angled features.

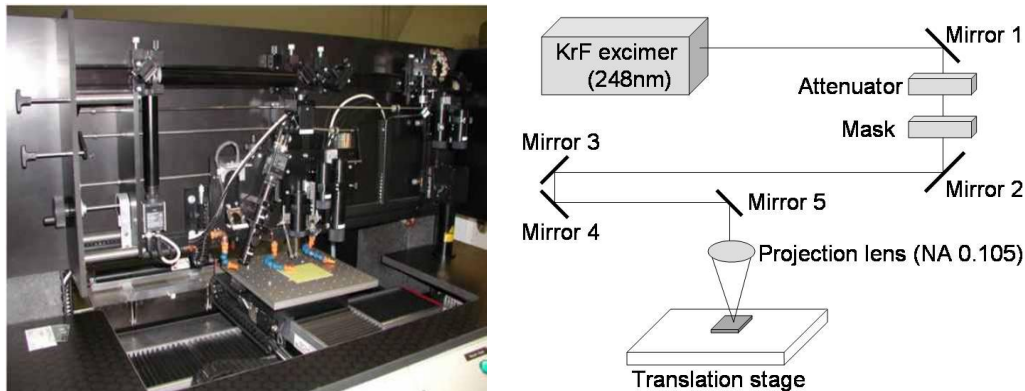


Fig. 1: picture of the laser ablation set-up; scheme of the optical path of the KrF excimer laser.

Different polymer materials are tested for the optical layer. Truemode Backplane™ Polymer (Exxelis Ltd., United Kingdom) is a highly cross-linked acrylate-based material that can be patterned with UV-photolithography. The UV-exposure however has to be done in a nitrogen environment with photo-mask in proximity mode. Fully cured Truemode layers can also be patterned with laser ablation, which can be done in a standard environment. Truemode shows excellent ablation properties resulting in ablated structures with low surface roughness. Dry Truemode (Exxelis Ltd., United Kingdom) is a variant of Truemode, which can be patterned with UV-lithography in standard environment with photo-mask in contact mode.

## 3. MULTILAYER OPTICAL INTERCONNECTIONS

### 3.1 Multimode waveguides

The polymer optical layer, which consists of a cladding-core-cladding stack, is applied onto the FR4 substrate with use of spin-coating. The multimode waveguide core features are UV-defined for the Dry Truemode material and laser ablated for the Truemode material. The ablated waveguides have an average propagation loss of 0.12dB/cm at 850nm<sup>5</sup>,



which is slightly higher than the values obtained for photo-lithographically defined ones. The advantage of the ablation process is the fact that design changes can be adopted in a very flexible way, whereas this would require the fabrication of a new mask in case photo-lithography is used. Fig.2 shows a picture of the input facet of an array of laser ablated (a) and photo-lithographically defined (b) waveguides. The waveguides have a cross-section of  $50\mu\text{m}\times 50\mu\text{m}$  on a pitch of  $125\mu\text{m}$  and  $250\mu\text{m}$ . There is always a certain degree of tapering during the ablation which gives a slight trapezoidal form to the ablated waveguide cores.

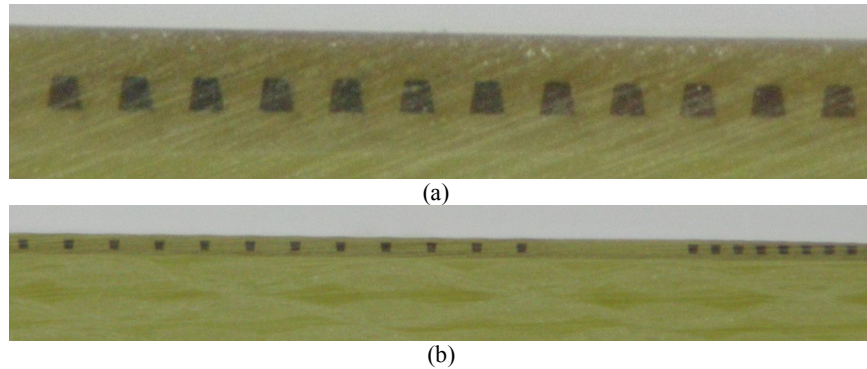
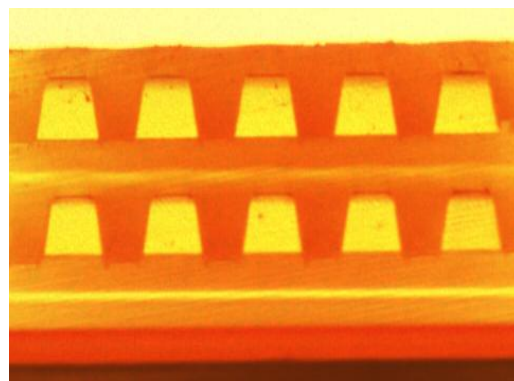


Fig. 2: (a) shows a picture of the input facet of an array of laser ablated waveguides on pitch  $125\mu\text{m}$  in Truemode; (b) shows the input facet of an array of photolithographic waveguides on pitch  $125\mu\text{m}$  and  $250\mu\text{m}$  in Dry Truemode.



(a)



(b)

Fig. 3: (a) shows a cross-section of a two layer structure with ablated waveguides in Truemode where SU8 is used as planarization layer; (b) picture of the input facet of a two layer structure with ablated waveguides in Truemode where the alignment marks are placed on the lower cladding layer of the bottom optical layer. The waveguides have a cross-section of  $50\mu\text{m}\times 50\mu\text{m}$  on pitch  $125\mu\text{m}$ .

If we go one step further and look at two layer optical structures, where two optical layers are stacked on top of each other, it is clear that the alignment between the two layers is critical. The alignment between waveguides in top and bottom layer has to be accurate enough if we want to couple light from one layer to the other with the use of coupling

structures. The FR4 substrate has a high surface roughness and suffers from warpage. The alignment marks are therefore placed either on a planarization layer or on the lower cladding layer of the bottom optical layer. In case photolithography is used the achievable alignment accuracy is in accordance with the alignment accuracy of the used mask aligner. The ablated waveguides are structured in each optical layer separately. The achievable alignment accuracy is for both cases  $\leq 5\mu\text{m}$ , which is in accordance with the results obtained from a numerical study using non-sequential ray-tracing<sup>6</sup>. The experimental results are shown in Fig.3.

### 3.2 Coupling structures

The use of efficient coupling structures is critical for the performance of the system. We propose the use of  $45^\circ$  micro-mirrors, which can be ablated into the optical layer with tilted excimer laser beam. The mirrors are integrated with the waveguides, and are aligned with respect to the waveguides with the use of the before mentioned alignment marks. There is always a certain degree of tapering during the ablation which can be measured and consequently corrected for.

The cavity that is made during the ablation contains two interfaces with a different slope. The slope of the first interface, which is first hit by the light beam propagating through the waveguide, is steeper than the second one because of the tapering that occurs during the ablation. Both interfaces can be used to deflect the light beam. In the first case, the light deflection occurs through the total internal reflection at the polymer-air interface. The other mirror configuration is a metallized  $45^\circ$  mirror<sup>7</sup>. The tilt angle of the excimer laser beam has been optimized to obtain a  $45^\circ$  mirror facet for both cases. The ablation parameters (pulse energy and repetition rate) and size of the mask have been optimized to ensure minimal surface roughness of the ablated facet.

The fabrication of the TIR mirror requires only one processing step. The  $45^\circ$  TIR facet is ablated with the laser beam under the suitable tilt angle and can be immediately used. The light beam that propagates in the plane of the optical layer in the waveguide is deflected over  $90^\circ$  when it strikes the  $45^\circ$  polymer-air interface. TIR mirrors can only be used in a multilayer structure when a metal coating is applied on the mirror facet. The ablated trench will be filled with cladding material when the lower cladding layer of the next optical layer is spin-coated on top of the bottom optical layer. The light beam will however still be deflected over  $90^\circ$  because of the presence of the Au-coating. Experimental results are shown in Fig.4. The right picture shows the top view of a Au-coated TIR mirror. The sample has to be tilted in a suitable way in the vacuum chamber to allow for the deposition of Au on the TIR facet.

The fabrication of the metallized mirror requires three processing steps, as shown in Fig. 5. First, the  $45^\circ$  facet is ablated. The facet is subsequently coated with a 50-nm-thick layer of sputtered Ti, to improve adhesion to the polymer material, and a 100-nm thick layer of Au, to guarantee a high reflectivity. The last step consists of the filling of the ablated trench with cladding material. The experimental results shown in Fig. 6 clearly show the good coverage of the facet with the metal coating and the good filling of the ablated area. The sample is tilted in the vacuum chamber with the use of a suitable holder, this to avoid the deposition of metal on the TIR facet which is in this case not under a  $45^\circ$  angle.

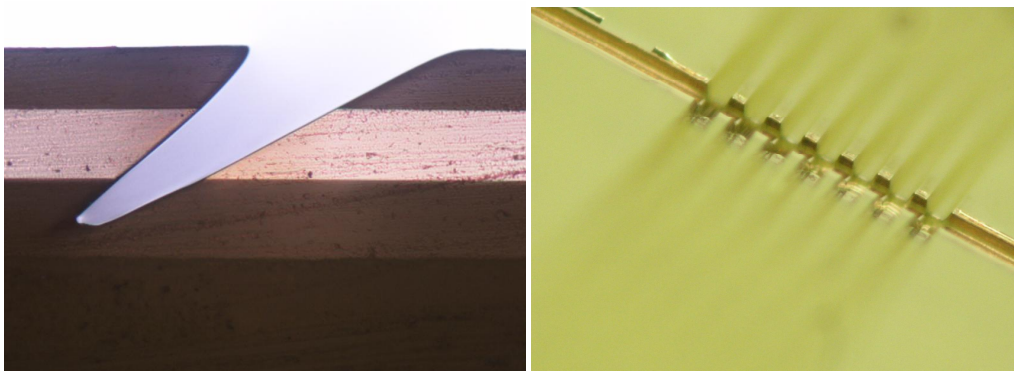


Fig. 4: the left picture shows a cross-section of a laser ablated TIR mirror; the right picture shows a top view of a metallized TIR mirror.

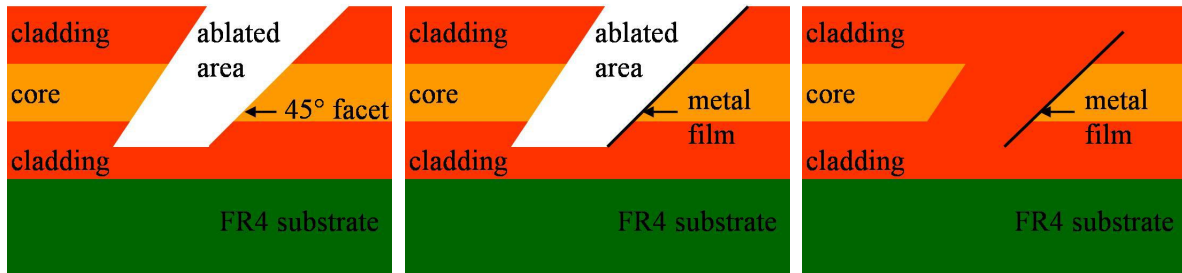


Fig. 5: Scheme of the different processing steps that are used for the fabrication of the metallized 45° mirrors.

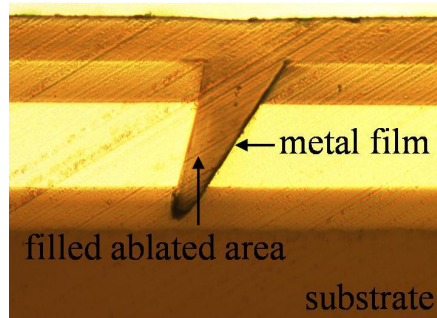


Fig. 6: cross-section of a metallized 45° micro-mirror. The mirror facet is in this case coated with a thick Au-coating to allow us to evaluate the coverage of the TIR facet.

### 3.3 Out-of-plane coupling

Both the metallized TIR mirrors and the metallized 45° mirrors can be used in a two layer structure to couple the light between the two layers or out of the plane of the optical layers. The out-of-plane coupling configuration can be for instance used to couple light from a VCSEL array into the waveguides or from the waveguides to a photo-detector array. The mirrors are ablated in each layer separately and are aligned with respect to the waveguides with the help of the alignment marks on the lower cladding layer of the bottom optical layer. Fig.7 shows the scheme and experimental realization of an out-of-plane coupling structure in case metallized 45° mirrors are used to deflect the light beam. The same procedure is followed in case metallized TIR mirrors are used.

### 3.4 Inter-layer coupling

The mirrors can also be used to couple light between the waveguides in top and bottom layer. Two different cases can be considered: one where the propagation direction is preserved and one where it is turned over 180°. Fig.8 shows schemes and experimental realizations for both cases. The alignment procedure for the first configuration, where the propagation direction is preserved, is the same as for the out-of-plane coupling structure. The achievable alignment accuracy is  $\leq 5\mu\text{m}$ . The alignment between the mirrors in the other inter-layer coupling configuration is more complicated. The center of the mirror in top and bottom layer should coincide. The board however has to be rotated over 180° for the ablation of the mirror in the top layer. The alignment between the mirrors will therefore not only depend on the followed alignment procedure but also on the reproducibility of the thickness of the cladding and core layers in top and bottom optical layer. The accuracy on thickness of the Truemode layer is  $5\mu\text{m}$  to  $10\mu\text{m}$ , and a deviation in the layer thickness gives a certain misalignment. The achievable alignment accuracy is approximately  $10\mu\text{m}$  but depends on the layer thicknesses<sup>6</sup>.

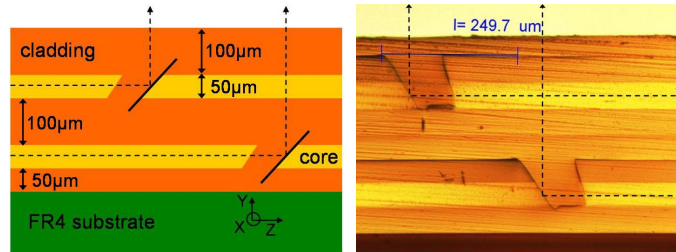


Fig. 7: the left picture shows a scheme of a two layer out-of-plane coupling structure; the right picture shows a cross-section of an experimental realization. The pitch between the outcoupled spots is  $250\mu\text{m}$ .

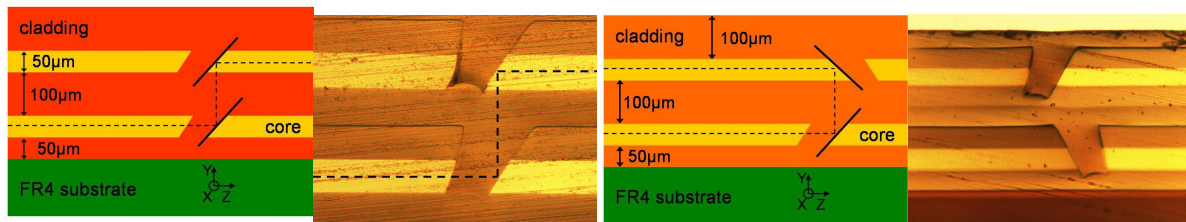


Fig. 8: the two left pictures show the scheme and experimental realization of an inter-plane coupling structure where the propagation direction of the light beam is conserved; the two right pictures show a scheme and experimental realization of an inter-plane coupling structure where the propagation direction of the light beam is turned over  $180^\circ$ . The  $45^\circ$  mirror facets are in this case not metallized.

#### 4. MEASUREMENT RESULTS

Loss measurements have been carried out on a PCB with one optical layer, which is integrated on top of the substrate. The optical layer contains arrays of ablated multimode waveguides and an ablated TIR mirror in Truemode material. The measurements are carried out at a wavelength of  $850\text{nm}$ . Light is coupled into the waveguides in-plane with a multimode optical fiber with a core diameter of  $50\mu\text{m}$  and a numerical aperture (NA) of 0.2. The input facet of the waveguides is polished manually. The light that is deflected at the TIR mirror is detected at the output facet with a multimode optical fiber with core diameter  $100\mu\text{m}$  and NA 0.29. The Truemode waveguides have NA 0.3 and an average propagation loss of  $0.12\text{dB/cm}$ . The measurements are carried out on an uncoated TIR mirror. The measurement results give an average coupling loss of  $-2.55\text{dB}$  for the entire link (coupling into the Truemode waveguides, propagation through the  $2\text{cm}$  long waveguide,  $90^\circ$  deflection at the TIR facet and outcoupling at the output facet towards the fiber). Fig.9 shows a lateral scan of the coupling efficiency of a light spot coupled out at the TIR mirror facet. The right picture shows the spot that is coupled at at the TIR mirror facet with use of a red laser light source.

Light has also been coupled in vertically with a single mode fiber (SMF-28) at the TIR mirror to get an idea of the behavior of the TIR mirror when it is used at the transmitter side. The outcoupled light is detected in-plane with multimode optical fiber with core diameter  $100\mu\text{m}$  and NA 0.29. The measurements give an average loss of  $-1.16\text{dB}$  over the entire link.

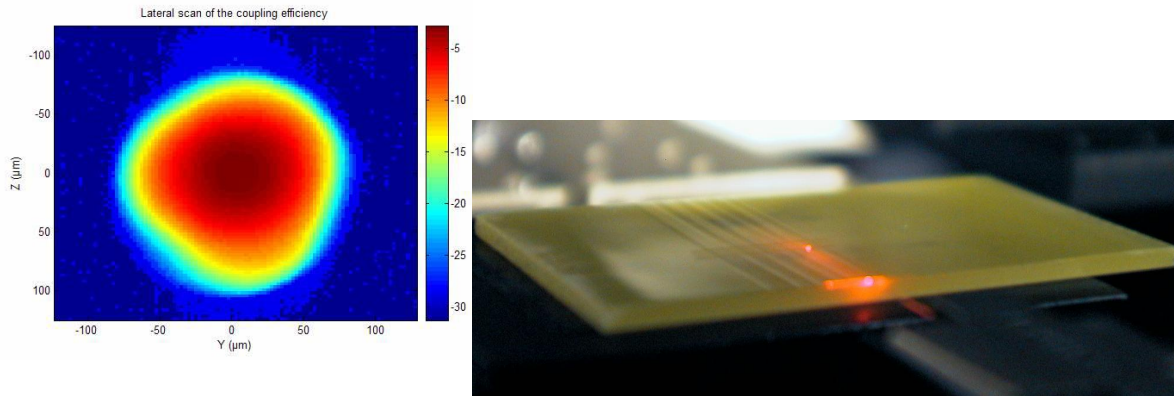


Fig. 9: the left picture shows a lateral scan of the coupling efficiency of a light spot coupled out at the TIR mirror facet; the right picture shows a picture of the outcoupled lightspot with use of a red light source.

## 5. CONCLUSIONS

In this paper we have shown the use of multilayer optical interconnections to provide more flexibility in the routing of optical signals on printed circuit boards and to fully exploit the characteristics of 2D opto-electronic elements such as VCSEL and photo-detector arrays. Further work has to be carried out on the characterization of the metal-coated mirrors in order to come to a demonstrator board.

## ACKNOWLEDGEMENTS

Nina Hendrickx would like to acknowledge the Institute for the Promotion of Innovation by Science and Technology in Flanders (IWT Flanders) for financial support. Jürgen Van Erps acknowledges the FWO for financial support. This work was carried out within the framework of the network of excellence on micro-optics (NEMO), supported by the European Commission through FP6 program.

## REFERENCES

- <sup>1</sup> D. Miller, H. Ozaktas, "Limit to the bit-rate capacity of electrical interconnects from the aspect ratio of the system architecture," *J. of parallel and distributed computing* **(41)**, pp. 42-52, 1997
- <sup>2</sup> El-Hang Lee, S. G. Lee, B. H. O, S. G. Park, K. H. Kim, "Fabrication of a hybrid electrical-optical printed circuit board (EO-PCB) by lamination of an optical printed circuit board (O-PCB) and an electrical printed circuit board (E-PCB)", *Proc. of SPIE Vol. 6126, 61260L*, (2006)
- <sup>3</sup> A. Glebov, M. G. Lee, S. Aoki, D. Kudzuma, J. Roman, M. Peters, L. Huang, D. S. Zhou, and K. Yokouchi, "Integrated Waveguide Microoptic Elements for 3D Routing in Board-Level Optical Interconnects," *Proceeding SPIE Vol. 6126, 61260N*, 2006
- <sup>4</sup> G. Van Steenberge et al, "MT-compatible laser ablated interconnections for optical printed circuit boards," *J. Lightwave Technology* **22(4)**, pp. 2083-2090
- <sup>5</sup> G. Van Steenberge, N. Hendrickx, E. Bosman, J. Van Erps, H. Thienpont, and P. Van Daele, "Laser Ablation of Parallel Optical Interconnect Waveguides," *Photonics Technology Letters* **18(9)**, May 2006
- <sup>6</sup> N. Hendrickx, J. Van Erps, G. Van Steenberge, H. Thienpont, P. Van Daele, "Tolerance analysis for multilayer optical interconnections integrated on a printed circuit board," *Journal of Lightwave Technology* **25(9)**, pp. 2395-2401, September 2007
- <sup>7</sup> N. Hendrickx, J. Van Erps, G. Van Steenberge, H. Thienpont, P. Van Daele, "Laser ablated micro-mirrors for PCB-integrated optical interconnections," *Photonics Technology Letters* **19(11)**, pp. 822-824, June 2007

